

# Turbulence Modelling for Smoothed Particle Hydrodynamics



K T Prajwal Prathiksh

*Dual Degree Project (Stage II) - Presentation*

Supervisor: Prof. Prabhu Ramachandran

Department of Aerospace Engineering  
Indian Institute of Technology Bombay

June 30<sup>th</sup>, 2023

# Introduction

- **Turbulent Flow**

- Characterization
  - High Reynolds number flows
  - Random spatial & temporal velocity fluctuations
  - Rotational & 3D velocity field
  - Large mixing capacity of the flow
  - Chaotic nature of solutions

- Modelling

- Lacks analytical solutions except for simple cases
- CFD simulations required for complex flows
- Typical modelling techniques
  - Governing equations → Averaged or filtered
  - Closure problem → Fluctuating components modelled using mean flow properties
  - Stochastic methods
- Models mostly based on Eulerian framework

- **Lagrangian Modelling – SPH**

- No background mesh
- Handles large deformations, complex boundary dynamics
- Simplified model implementation
- Highly & efficiently parallelizable

# Project Objectives

- Turbulence Modelling in SPH
  - Lacks **robust & accurate** models
  - Shortcomings of current models
    - Cannot be **generalized** to various types of turbulence-based problems
    - Issues in scaling to 3D turbulent flows
      - Accuracy & computational constraints
    - Boundary conditions & treatment not well established
- Project Objective
  - Review state of the art turbulence models in SPH
  - Document advantages & disadvantages of the major categories of models
  - Identify **representative schemes** from each category
  - Analyze & study their performance for high Reynolds number ( $Re$ ) flows
  - Attempt at improving their accuracy & robustness using recent developments in SPH

**Existing  
Models**

**Expected  
Outcome**

# Post-Simulation Analysis

- Energy spectral density
  - Velocity field over a grid generated using suitable **interpolation** of the particle velocity data<sup>[1]</sup>
  - Fourier transform of the velocity field → Velocity spectrum as a function of the wave-number
  - Energy spectrum computed from the velocity spectrum
- Velocity gradient-based metrics
  - Iso-vorticity surfaces, Q-criterion, Δ-criterion, etc.
  - Most of the definitions for a vortex → **Not objective** & suitable for studying the flow (esp. 3D flow)<sup>[2]</sup>
- Lagrangian coherent structures (LCS)
  - Local velocity fluctuations do not induce noise in LCS
  - FTLE is **formulated** in the Lagrangian framework → Better identification of LCSs
  - Provides flexibility in its formulation<sup>[3]</sup>
    - Backward-in-time FTLE can be computed using limited resources during run-time concurrently
    - Forward-in-time FTLE can only be computed during post-processing
    - Easily parallelizable

[1] Y. Shi, X. X. Zhu, M. Ellero, and N. A. Adams, "Analysis of interpolation schemes for the accurate estimation of energy spectrum in Lagrangian methods," *Comput. Fluids*, vol. 82, pp. 122–131, 2013, doi: 10.1016/j.compfluid.2013.05.003.

[2] G. Haller, "An objective definition of a vortex," *J. Fluid Mech.*, vol. 525, pp. 1–26, 2005.

[3] P. N. Sun, A. Colagrossi, S. Marrone, and A. M. Zhang, "Detection of Lagrangian Coherent Structures in the SPH framework," *Comput. Methods Appl. Mech. Eng.*, vol. 305, pp. 849–868, 2016, doi: 10.1016/j.cma.2016.03.027.

# Energy Spectral Analysis

- Implementation
  - Interpolated vel. Field → Fourier Transform (numpy.fft.fftn)
  - $E_i(k) \rightarrow 1D E(k)$ : Integrating over sphere, between limits  $k \in (0, k_{max})$
- Test Case: Expected decay rate =  $2\gamma$

$$v_x = - \sum_{i=1}^N i^{-\gamma} \cos(2\pi i x) \sin(2\pi i y)$$

$$v_y = \sum_{i=1}^N i^{-\gamma} \sin(2\pi i x) \cos(2\pi i y)$$

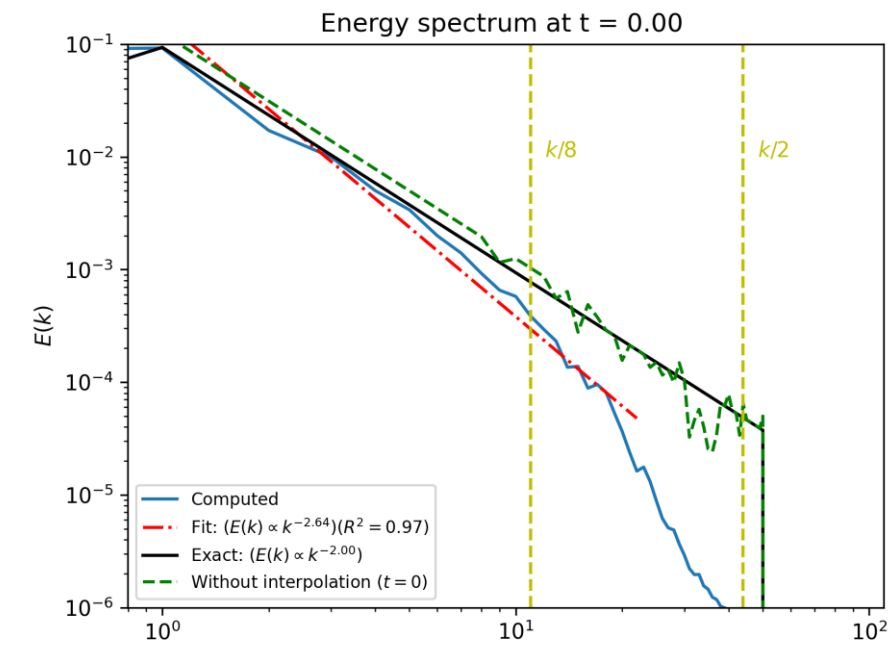


**Fig:** Scalar  $E(k)$  for 2D case with  $\gamma = 1, N = n_x/2$

- Observations:
  - Computation without interpolation → 'Best'-case
  - Interpolation → Energy captured at higher  $k$  is reduced
  - 'Low-pass' filter behaviour

# Energy Spectral Analysis

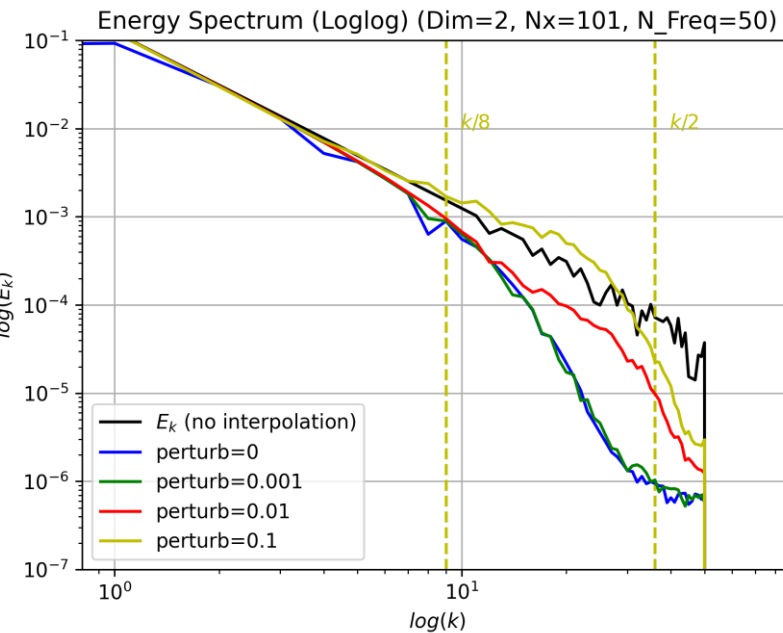


**Fig:** Scalar  $E(k)$  for 2D case for various perturbation amplitudes

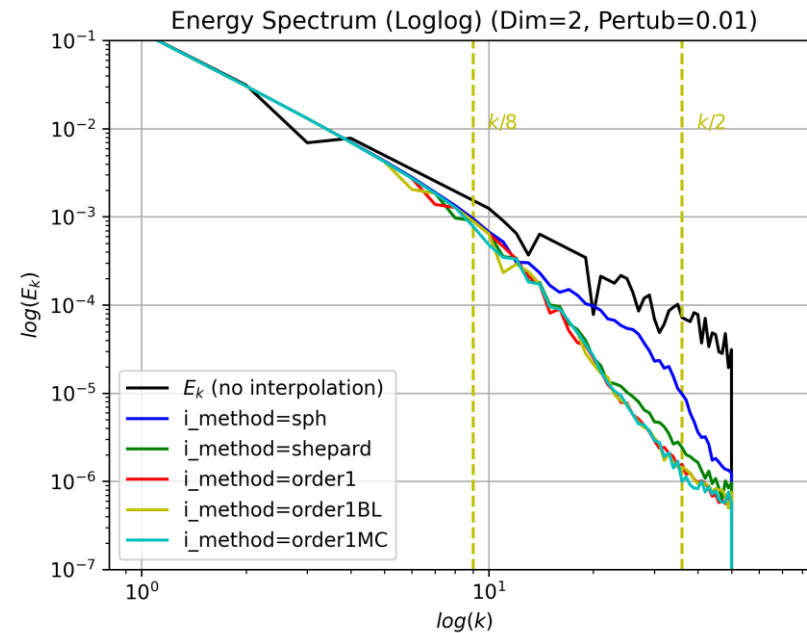


**Fig:** Scalar  $E(k)$  for 2D case for various interpolation methods

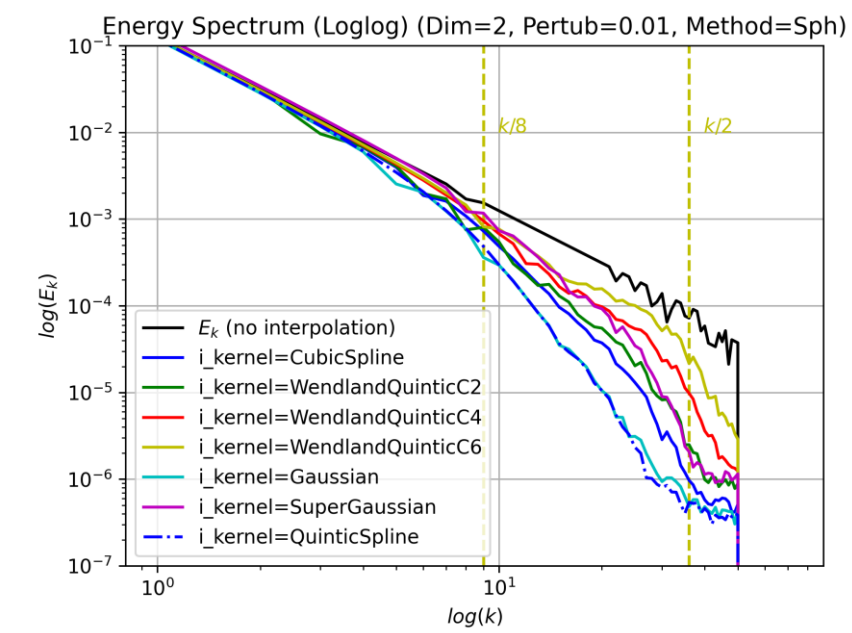


**Fig:** Scalar  $E(k)$  for 2D case for various kernels

## Observations

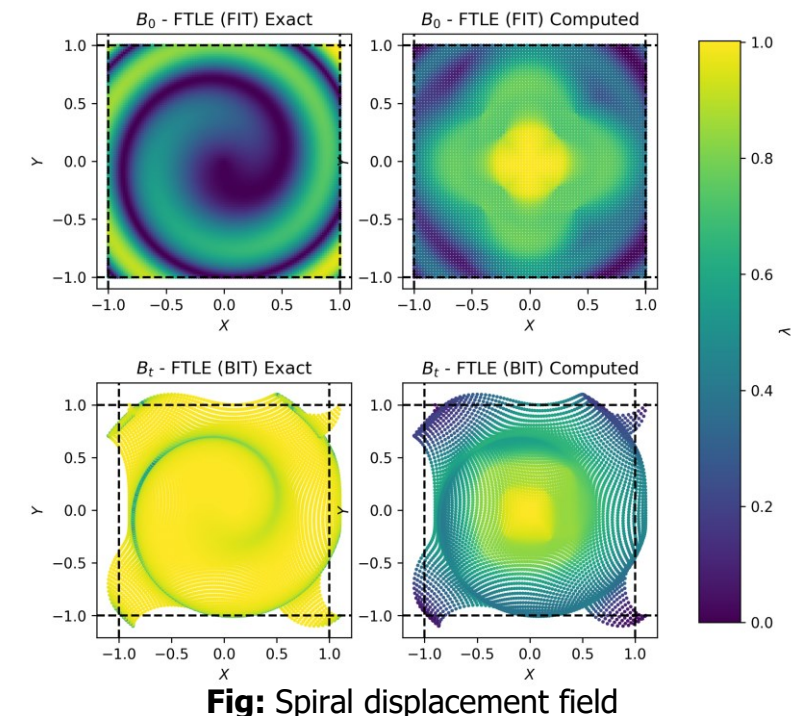
- Disorder in particle spacing: Counts effect of reduced energy in higher  $k$
- Interpolation method: **sph** counts effect of reduced energy the most
- Kernels: **WendlandQuinticC6** counts effect of reduced energy the most
- Resolution: Improves accuracy throughout

# Finite-time Lyapunov Exponent (FTLE) Field Analysis

- Implementation
  - Work of Sun, Colagrossi et al. 2016
  - Define  $\mathbb{F}_{t_i}^{t_f}(x)$ : Function of  $x$  of particles at two time-instances
  - Calculate Cauchy-Green tensor  $\mathbb{C}_{t_i}^{t_f}(x)$  field
  - Calculate max./min. eigenvalue of the tensor field
- Test-Case: Spiral displacement field

$$X = x + 0.1 \cos(2\pi r^2), \quad Y = y + 0.1 \sin(2\pi r^2), \quad r = \sqrt{x^2 + y^2}$$

- Observations
  - Current implementation → Qualitative results only
  - Not as accurate either
  - Consider implementation of tracer particles, or in situ FTLE computation for improved capturing of LCSs



**Vid:** [FIT - FTLE](#). (Rep: Brunton 2022)

[1] P. N. Sun, A. Colagrossi, S. Marrone, and A. M. Zhang, "Detection of Lagrangian Coherent Structures in the SPH framework," *Comput. Methods Appl. Mech. Eng.*, vol. 305, pp. 849–868, 2016, doi: 10.1016/j.cma.2016.03.027.

[2] S. L. Brunton (2022, February 11), *Lagrangian Coherent Structures (LCS) in unsteady fluids with Finite Time Lyapunov Exponents (FTLE)*

# Turbulence Models

- Surveyed research papers detailing work on turbulence models for SPH (c. 2000 – 2022)
- Classified 5 major categories of turbulence models
- Identified the following representative schemes
- Devised a systematic, model-evaluation method to quantify order of convergence (OOC)
  - Identify OOC using TGV problem ( $t_f = 0.1$ ) :  $Re = [10^2, 10^3, 10^4]$  ;  $N = [25^2, 50^2, 100^2]$
  - Post-simulation analysis techniques:  $L_1$  error; energy-spectrum; velocity field

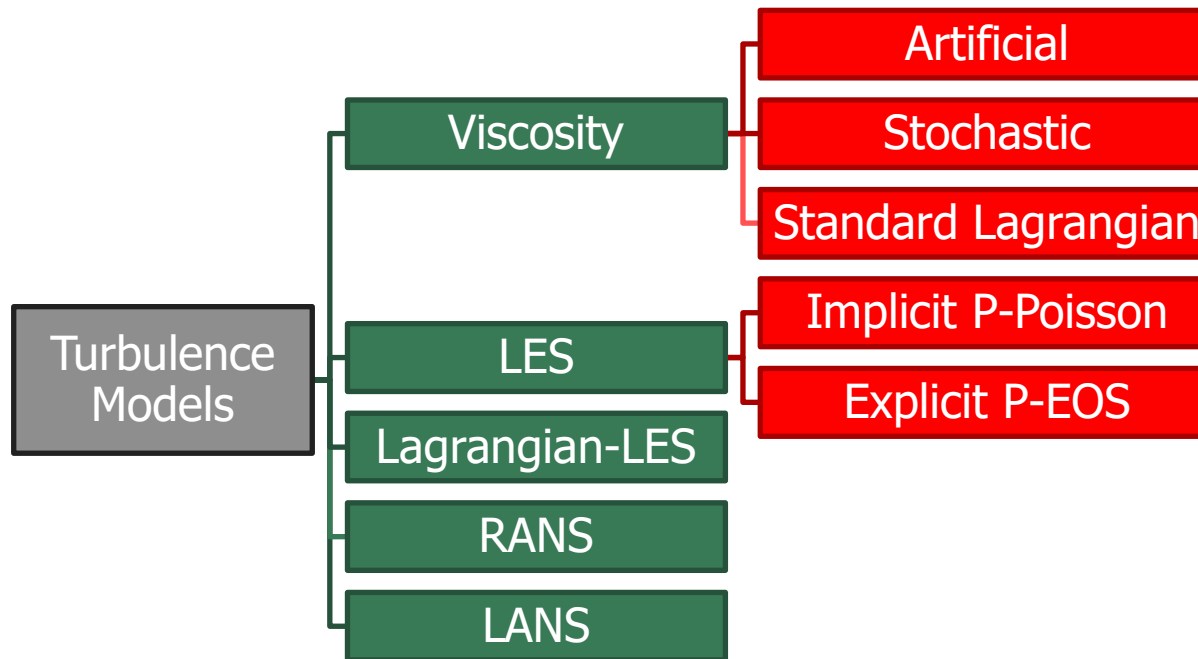


**Fig:** Chart of the major categories of turbulence models in SPH

Turbulence Model	Scheme Name	Reference
Viscosity – based <i>(Standard Lagrangian)</i>	Lagrangian with iterative PST and coupled_c viscosity formulation <b>(L-IPST-C)</b>	Negi et al. 2022
LES – based <i>(Explicit P-EOS)</i>	<b>SPH-LES</b>	Okrashevski et al. 2022
Lagrangian-LES – based	<b>δ-LES-SPH</b>	Antuono et al. 2021
RANS – based	<b>k – ε SPH</b>	Songdong Shao 2006
LANS - based	<b>SPH-ε</b>	J. J. Monaghan 2017

**Tab:** Representative turbulent SPH schemes

# Viscosity-based Model (L-IPST-C)

- Standard Lagrangian Formulation
  - No artificial viscosity added to the MOM eq.
  - $\nu \nabla^2 \nu$  implemented using coupled\_c formulation
  - Iterative particle shifting technique employed ( $10\Delta t$ )
    - Redistributions particles
    - Particle properties updated through Taylor-series exp.
  - Simulated multiple problems: TGV, Gresho vortex, & Kelvin-Helmholtz ( $Re = 10^2$ )
  - Used RK2 integrator

- **Comments**
  - Identified SPH approximation of operators to achieve second-order convergence (SOC)
  - Identified the optimum kernel and kernel radius for SOC
  - Recommended to use density as a **fluid property** instead of summation density
  - Recommended scheme observed to be SOC for a wide variety of problems

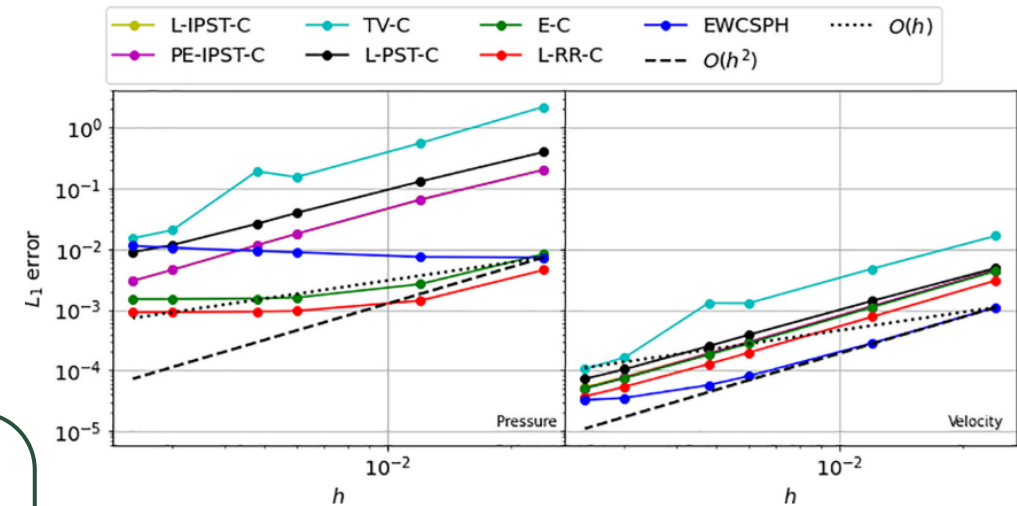


**Fig:** Convergence rates for pressure (left) and velocity (right) of different variants of SOC schemes. (Rep: Negi2022)

# Viscosity-based Model (L-IPST-C) Analysis

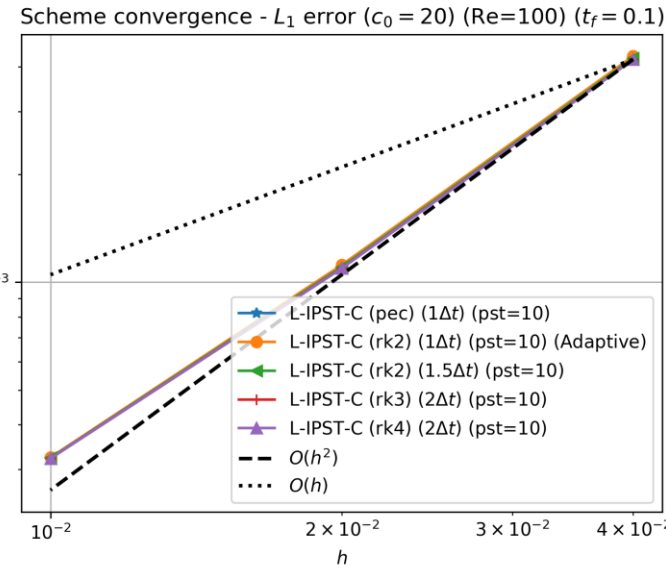


**Fig:** Convergence of the L-IPST-C scheme for various time-integrators ( $Re = 10^2$ )

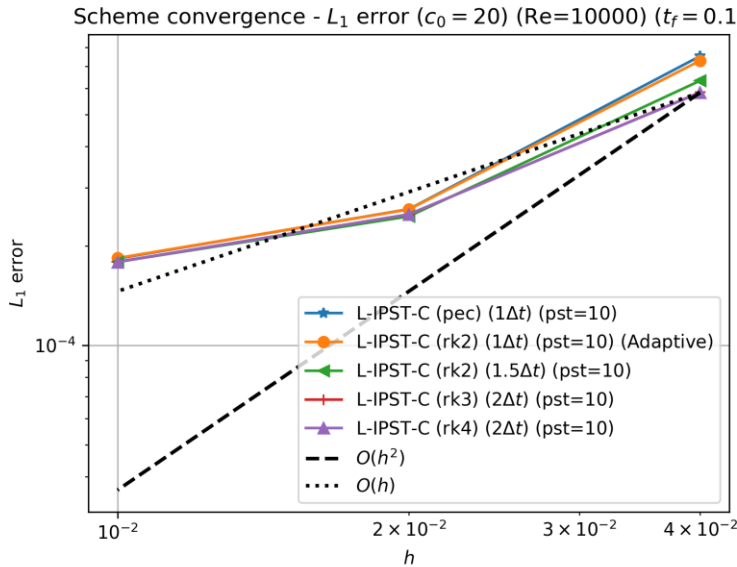


**Fig:** Convergence of the L-IPST-C scheme for various time-integrators ( $Re = 10^4$ )

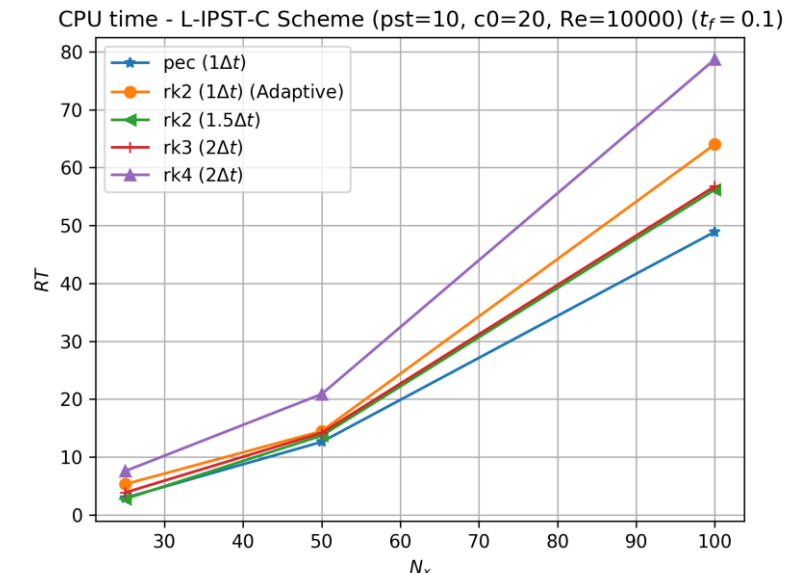


**Fig:** Run-time (in s) of the L-IPST-C scheme for various time-integrators ( $Re = 10^4$ )

## Observations

- Order of integrator: Negligible effect on OOC & magnitude of  $L_1$  error
- $\Delta t, CFL, c_s$  : More important factors for OOC
- Re increases: Scheme loses SOC
- Run-times: PEC integrator  $\approx 1.6 \times$  faster than the slowest, while maintaining accuracy & SOC

# Large-Eddy Simulation-based Model (SPH-LES)

- Explicit Pressure EOS-based Models<sup>[1]</sup>
  - Reinterpret SPH → Lagrangian quadrature technique for explicit LES
    - Kernel scale limits SPH's physical resolution → Unsuitable DNS alternative
  - Navier-Stokes (NS) eqs. → Spatially filtered
  - Compared multiple Smagorinsky models
    - (standard,  $\sigma$ , MCG-form)
  - Simulated 3D TGV ( $Re \approx 10^4$ ,  $N_i = 200^3 - 500^3$ )

- **Comments**
  - Smagorinsky models reduced averaged kinetic energy
  - Dissipation rates not predicted accurately
  - SPH can capture turbulence up to kernel scale (*high cost*)
  - Explicit SGS models remove kinetic energy → **Increases** energy deficit of standard SPH
  - "SGS models in SPH framework only degrade the quality of the subsonic turbulent flow approximation"<sup>[2]</sup>

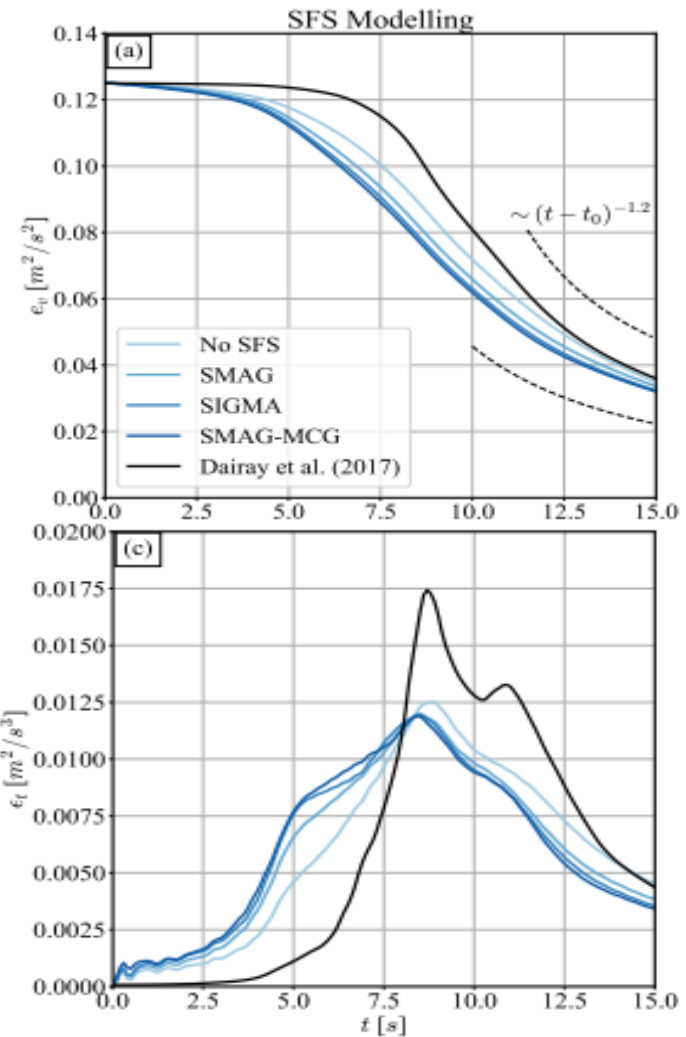


**Fig:** Density-weighted averaged kinetic energy (top), averaged dissipation rate (bottom). (Rep: Okrashevski et al)

[1] M. Okrashevski, N. Bürkle, R. Koch, and H.-J. Bauer, "Smoothed Particle Hydrodynamics Physically Reconsidered -- The Relation to Explicit Large Eddy Simulation and the Issue of Particle Duality," 2022, [Online].

[2] D. Rennehan, "Mixing matters," Mon. Not. R. Astron. Soc., vol. 506, no. 2, pp. 2836–2852, 2021.

# Large-Eddy Simulation-based Model (SPH-LES) Analysis

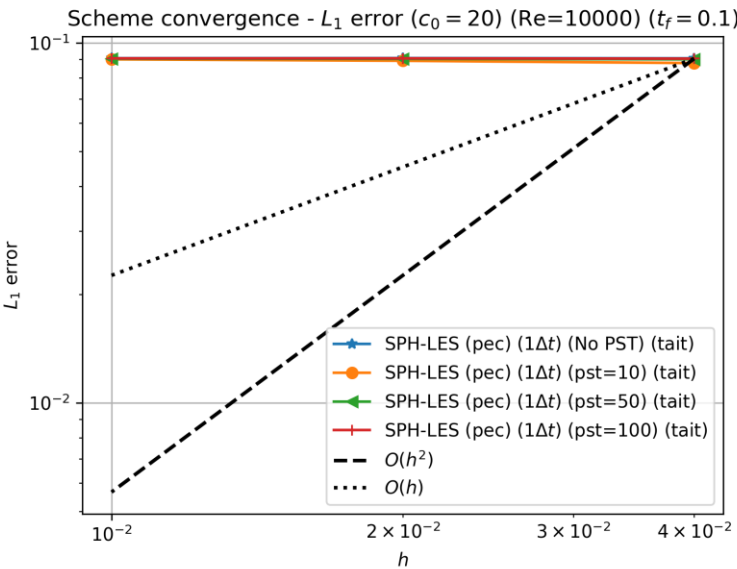


**Fig:** Convergence of the SPH-LES scheme for various  $f_{pst}$  values ( $Re = 10^4$ )

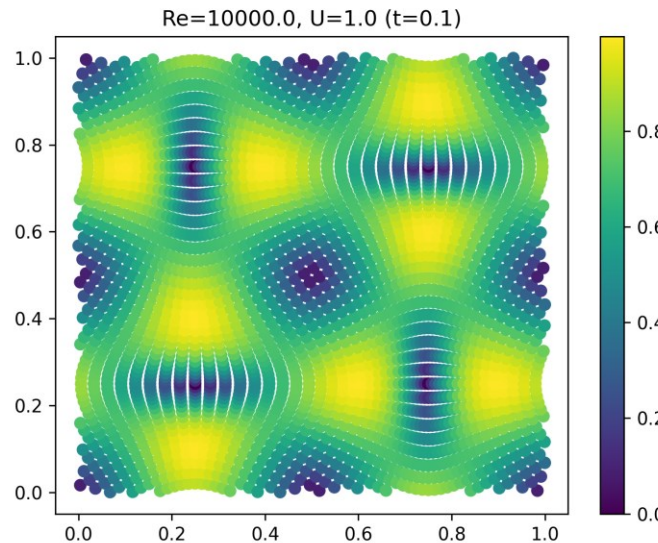


**Fig:** Velocity magnitude field for SPH-LES scheme ( $f_{pst} = None$ ) ( $Re = 10^4, N = 50^2$ )

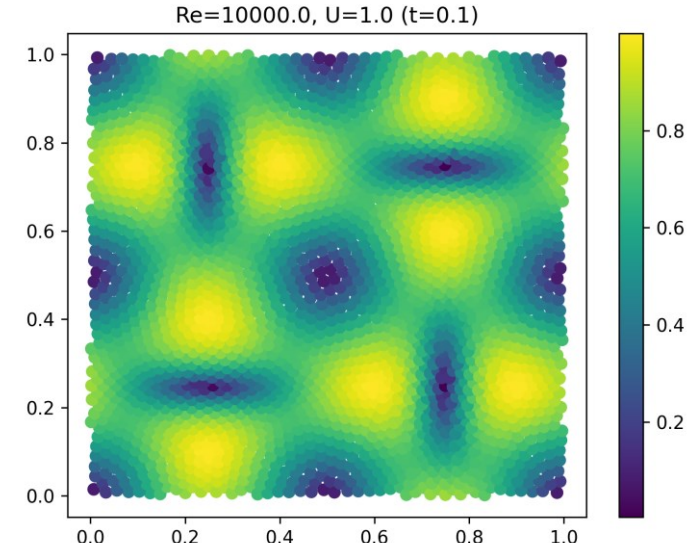


**Fig:** Velocity magnitude field for SPH-LES scheme ( $f_{pst} = 10$ ) ( $Re = 10^4, N = 50^2$ )

## Observations

- $f_{pst}$  :
  - No effect on the OOC or accuracy of the scheme
  - No PST  $\rightarrow$  Clustering of particles; Domain is no longer uniform
- $c_s$  : No effect on the OOC or accuracy

# Lagrangian LES-based Model ( $\delta$ -LES-SPH)

- Lagrangian form of LES<sup>[1,2]</sup>
  - Assumption: Weakly compressible flow
  - Lagrangian filter -  $\phi$  (compact support, even) introduced
  - $\phi$  decomposed into independent spatial & temporal components
  - Governing eqs. written using spatially filtered terms
    - Temporal terms of higher order neglected
    - Continuity eq. closed using Fick-like diffusion term
    - MOM eq. closed using Yoshizawa-model for the stress tensor
    - Considered  $\delta$ -SPH formulation
  - Simulated:
    - 2D TGV ( $Re \approx 10^3 - 10^6$ ,  $N_i \approx 10^3 - 10^6$ )
    - 3D homogenous turbulence ( $Re \approx 10^3$ ,  $N_i = 64^3 - 256^3$ )

- Comments
  - The model overcomes issues of spurious high-frequency noise & onset of tensile instability (High  $Re$  flows)
  - The energy spectra agrees well with theoretical decay rate
  - Wall functions need to be incorporated to deal with boundaries
  - Higher-order approach can significantly improve the performance

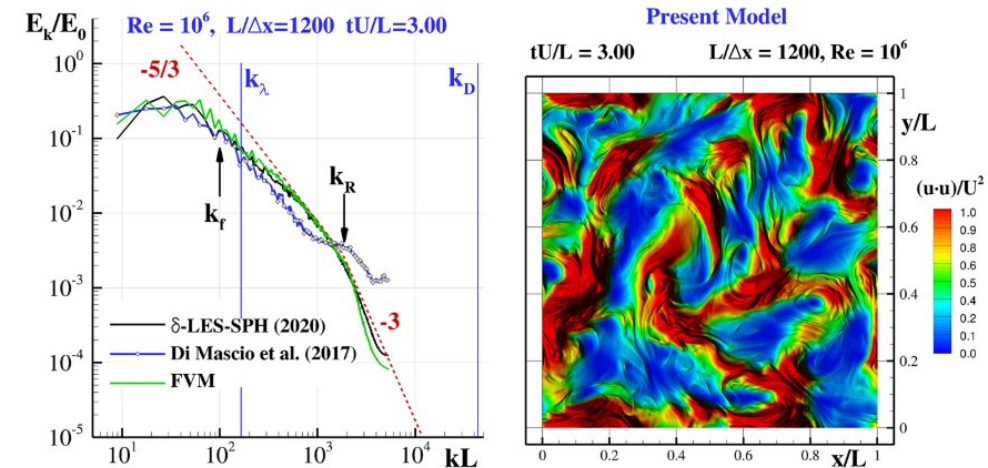


**Fig:** Energy spectrum (left),  $k$  field (right). (Rep: Antuono2021)

$$\begin{aligned} \frac{D\tilde{\rho}}{Dt} &= -\tilde{\rho}\langle\nabla\cdot\tilde{\mathbf{v}}\rangle + C_1 + C_2 \\ \frac{D\tilde{\mathbf{r}}}{Dt} &= \tilde{\mathbf{v}} \\ \tilde{P} &= F(\tilde{\rho}) \\ C_2 &\approx \nabla\cdot(\nu_\delta\nabla\tilde{\rho}) \end{aligned}$$

$$\begin{aligned} \frac{D\tilde{\mathbf{v}}}{Dt} &= -\frac{\langle\nabla\tilde{P}\rangle}{\tilde{\rho}} + \nu\langle\Delta(\tilde{\mathbf{v}})\rangle + \\ &(\lambda' + \nu)\langle\nabla(\nabla\cdot\tilde{\mathbf{v}})\rangle + M_1 + M_2 \\ M_2 &= \nabla\cdot\mathbf{T}_l = \nabla\cdot\left(-\frac{k^2}{3}\mathbf{I} - \right. \\ &\left.\frac{2}{3}\nu_t\text{Tr}[\tilde{\mathbf{S}}]\mathbf{I} + 2\nu_t\tilde{\mathbf{S}}\right) \end{aligned}$$

[1] A. Di Mascio, M. Antuono, A. Colagrossi, and S. Marrone, "Smoothed particle hydrodynamics method from a large eddy simulation perspective," Phys. Fluids, vol. 29, no. 3, 2017, doi: 10.1063/1.4978274.

[2] M. Antuono, S. Marrone, A. Di Mascio, and A. Colagrossi, "Smoothed particle hydrodynamics method from a large eddy simulation perspective. Generalization to a quasi-Lagrangian model," Phys. Fluids, vol. 33, no. 1, p. 015102, Jan. 2021, doi: 10.1063/5.0034568.

# Lagrangian LES-based Model ( $\delta$ -LES-SPH) Analysis

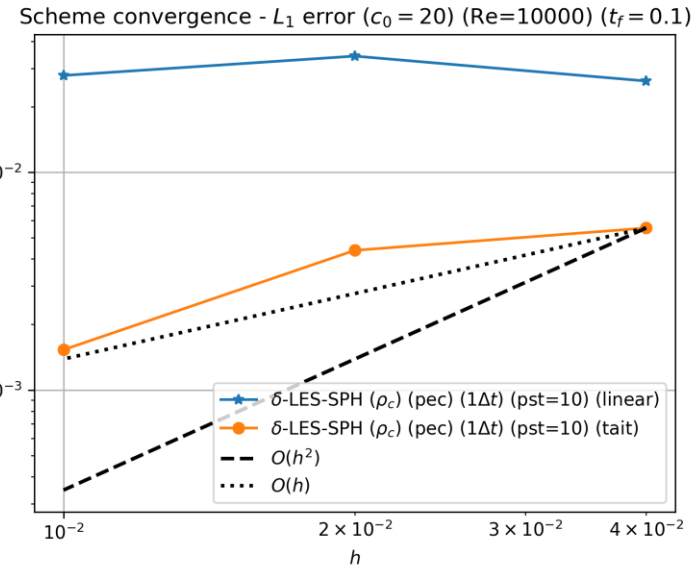


**Fig:** Convergence of the  $\delta$ -LES-SPH ( $\rho_c$ ) scheme for various equations of state ( $Re = 10^4$ )

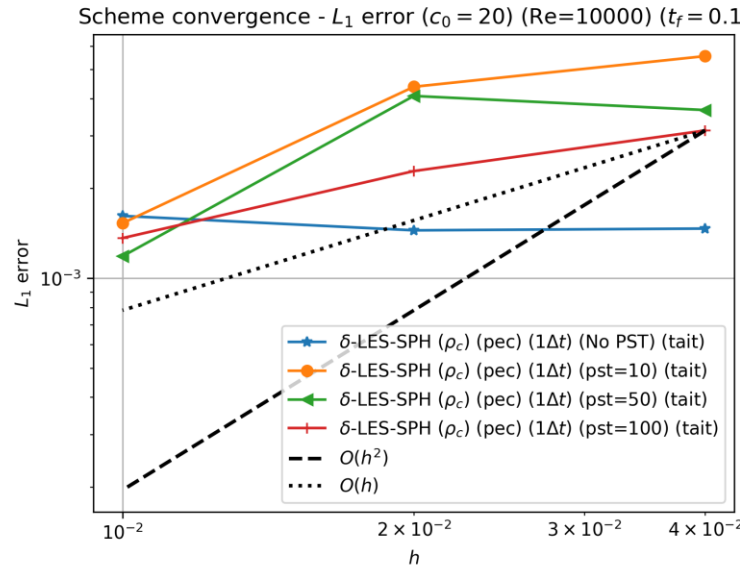


**Fig:** Convergence of the  $\delta$ -LES-SPH ( $\rho_c$ ) scheme various  $f_{pst}$  values ( $Re = 10^4$ )

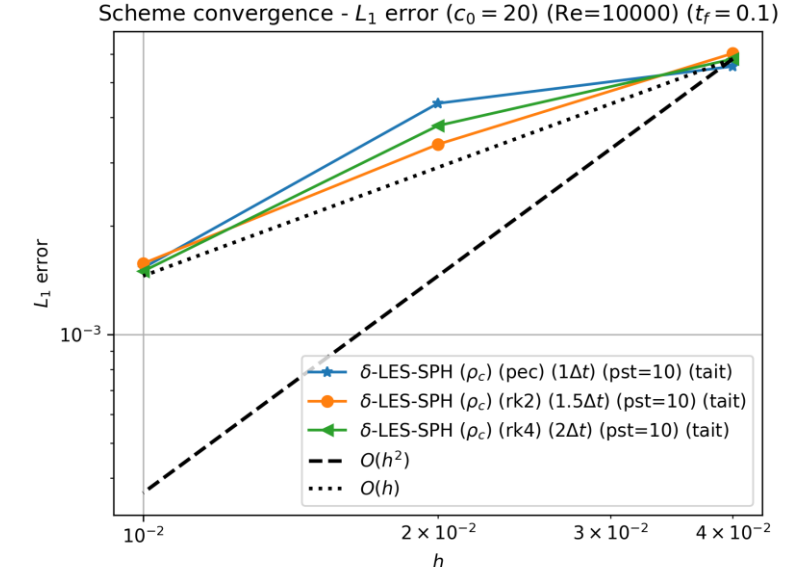


**Fig:** Convergence of the  $\delta$ -LES-SPH ( $\rho_c$ ) scheme various time integrators ( $Re = 10^4$ )

## Observations

- $\delta$ -LES-SPH ( $\rho_c$ ): Offers better OOC when used with [TaitEOS](#) than the other combinations
- $f_{pst}$ :
  - Magnitude of error is least when PST is disabled
  - OOC improves with PST as well as the [state](#) of the velocity field
- Integrator: RK2 offers the best OOC and is faster

# RANS-based Model ( $k - \epsilon$ SPH)

- $k - \epsilon$  Models<sup>[1,2]</sup>
  - Considered incompressible, **unsteady** RANS equations
  - Predictive-corrective time integrator
    - Requires **implicit** solution of pressure poisson eq
  - Simulated:
    - 2D wave breaking and overtopping of sloping wall<sup>[1]</sup> ( $Re \approx 10^6$ ,  $N_i = 6000$ )
    - 2D solitary wave propagating over a bottom-mounted barrier<sup>[2]</sup> ( $Re \approx 10^6$ ,  $N_i \approx 1.3 \times 10^5$ )

- **Comments**
  - Accurately tracks free-surfaces
  - $k - \epsilon$  coefficients (empirically derived from quasi-steady state) perform sub-optimally in transient flow
  - Model requires a sensitivity analysis for the turbulence model & spatial resolution for improved performance
  - Underpredicts max  $k$  & is sensitive to **initial seeding** of  $k$
  - Effects of viscous dissipation & numerical dissipation need to be balanced

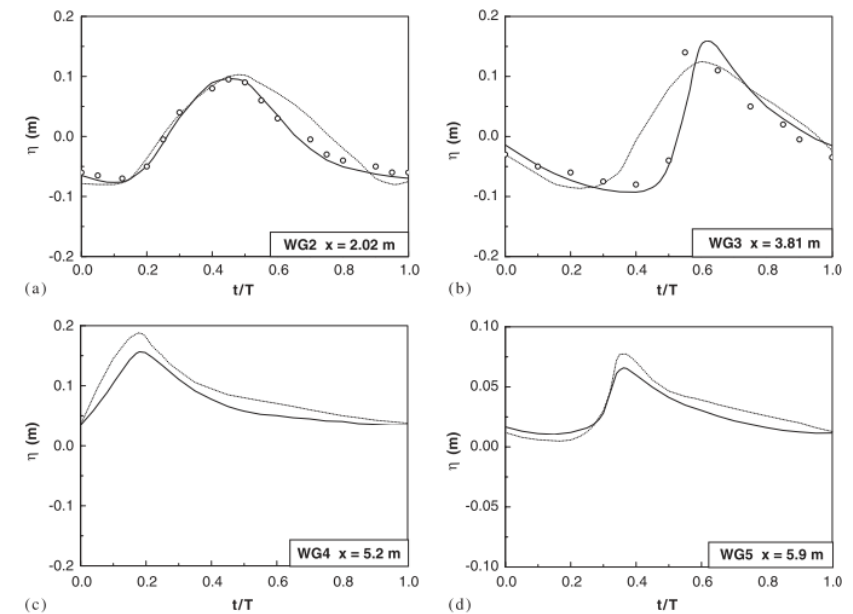


**Fig:** Water surface elevations. (Rep: Shao et al)c

$$\nu_t = c_d \frac{k^2}{\epsilon}$$

$$\frac{D k}{D t} = \nabla \cdot \left( \frac{\nu_t}{\sigma_k} \nabla k \right) + P_k - \epsilon$$

$$\frac{D \epsilon}{D t} = \nabla \cdot \left( \frac{\nu_t}{\sigma_\epsilon} \nabla \epsilon \right) + c_{1\epsilon} \frac{\epsilon}{k} P_k - c_{2\epsilon} \frac{\epsilon^2}{k}$$

$$P_k = 2\nu_t \langle \underline{S}, \underline{S} \rangle$$

[1] S. Shao, "Incompressible SPH simulation of wave breaking and overtopping with turbulence modelling," no. May 2005, pp. 597–621, 2006.

[2] D. Wang and P. L. F. Liu, "An ISPH with  $k-\epsilon$  closure for simulating turbulence under solitary waves," *Coast. Eng.*, vol. 157, no. July 2019, p. 103657, 2020, doi: 10.1016/j.coastaleng.2020.103657.

# RANS-based Model ( $k - \epsilon$ SPH) Analysis

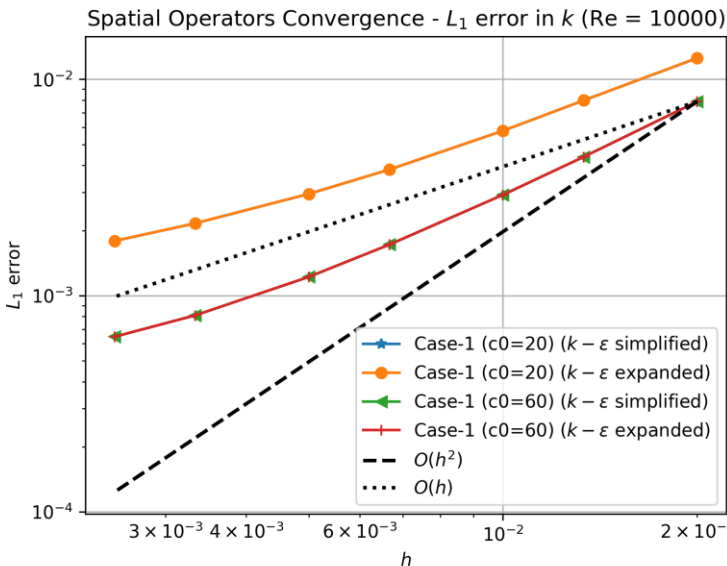


**Fig:** Convergence of the spatial operators -  $k$  transport equation (Test-case: 1) ( $Re = 10^4$ )

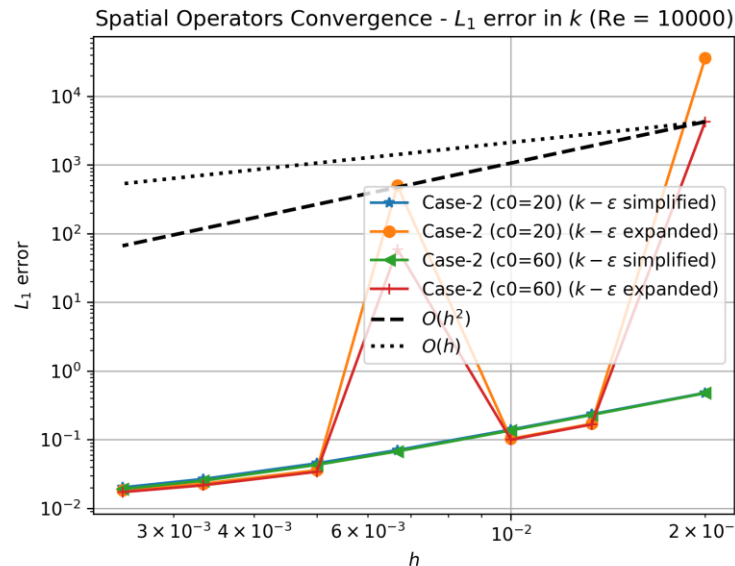


**Fig:** Convergence of the spatial operators -  $k$  transport equation (Test-case: 2) ( $Re = 10^4$ )

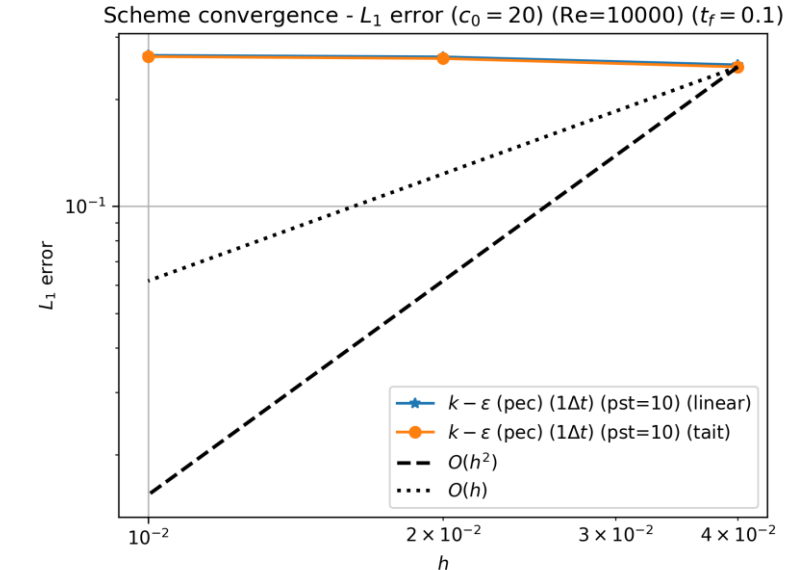


**Fig:** Convergence of the  $k - \epsilon$  SPH scheme for various equations of state ( $Re = 10^4$ )

## Observations

- $k - \epsilon$  SPH discretisation:
  - Variant with simplified transport equations is SOC
  - Increased speed of sound → Improved accuracy
- EOS:
  - Negligible effect on OOC & accuracy
  - TaitEOS better captures the velocity field
- $f_{pst}$ :
  - No effect on the OOC or accuracy of the scheme
  - No PST → Clustering of particles; Domain is no longer uniform

# LANS-based Model (SPH- $\epsilon$ )

- Lagrangian-averaged NS eqs. (LANS- $\alpha$ ) Models<sup>[1,2,3,4]</sup>
  - Lagrangian-averaging<sup>[1]</sup>: Performed at the level of **variational principle** from which NS eqs. are derived
    - $\alpha$  denotes scale of rapid fluctuations in the flow map
  - SPH- $\alpha$  model<sup>[2]</sup> → Initial models based on LANS- $\alpha$  eqs.
    - Particle transport → Smoothed velocity
    - MOM eq. solved iteratively
  - SPH- $\epsilon$  model<sup>[3,4]</sup> → Improvement of SPH- $\alpha$  model
    - Explicit MOM eq. with viscous term
  - Simulated 2D flow past a cylinder moving along a Lissajous curve<sup>[4]</sup> ( $Re \approx 10^3$ ,  $N_i \approx 10^4$ )

- **Comments**
  - **Bounded (no-slip)** flow implies  $\mathbf{v}$  is neither periodic/isotropic → Author prefers correlation functions over energy spectrum
  - Satisfactory results for velocity correlation functions, energy spectrum & mixing with half the particle resolution of DNS
  - Flows with larger Reynolds numbers & other boundary conditions, such as free surfaces need to be studied

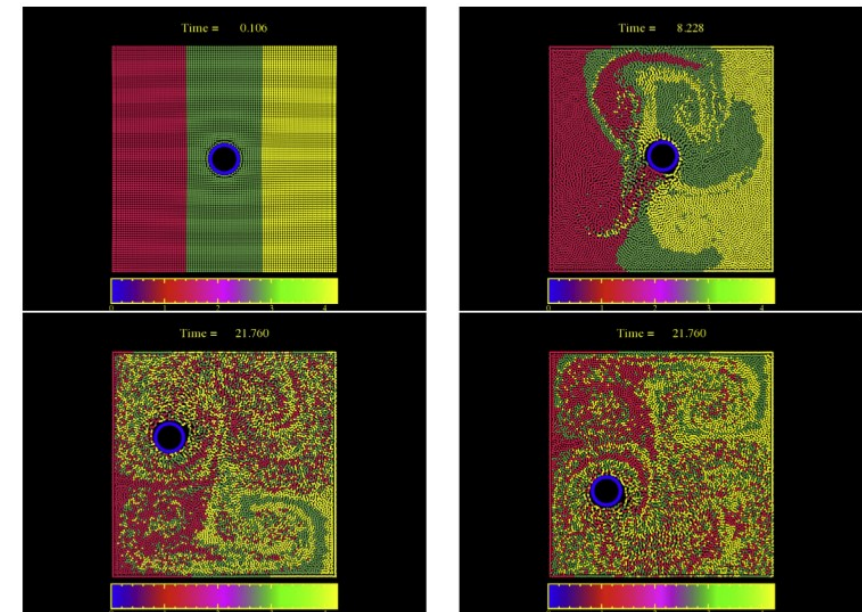


**Fig:** Stirring of coloured particles. (Rep: Monaghan2017)

$$\hat{\mathbf{v}}_i = \mathbf{v}_i - \varepsilon \sum_j \frac{m_j}{M_o} \mathbf{v}_{ij} K_{h',ij}$$

[1] J. E. Marsden and S. Shkoller, "Global well-posedness for the Lagrangian averaged Navier-Stokes (LANS- $\alpha$ ) equations on bounded domains," *Philos. Trans. R. Soc. A Math. Phys. Eng. Sci.*, vol. 359, no. 1784, pp. 1449–1468, 2001, doi: 10.1098/rsta.2001.0852.

[2] J. J. Monaghan, "SPH compressible turbulence," *vol. 852*, pp. 843–852, Apr. 2002, doi: 10.1046/j.1365-8711.2002.05678.x.

[3] J. J. Monaghan, "A turbulence model for smoothed particle hydrodynamics," *Eur. J. Mech. B/Fluids*, vol. 30, no. 4, pp. 360–370, 2011, doi: 10.1016/j.euromechflu.2011.04.002.

[4] J. J. Monaghan, "SPH- $\epsilon$  simulation of 2D turbulence driven by a moving cylinder," *Eur. J. Mech. B/Fluids*, vol. 65, pp. 486–493, 2017, doi: 10.1016/j.euromechflu.2017.03.011.

# LANS-based Model (SPH- $\epsilon$ ) Analysis

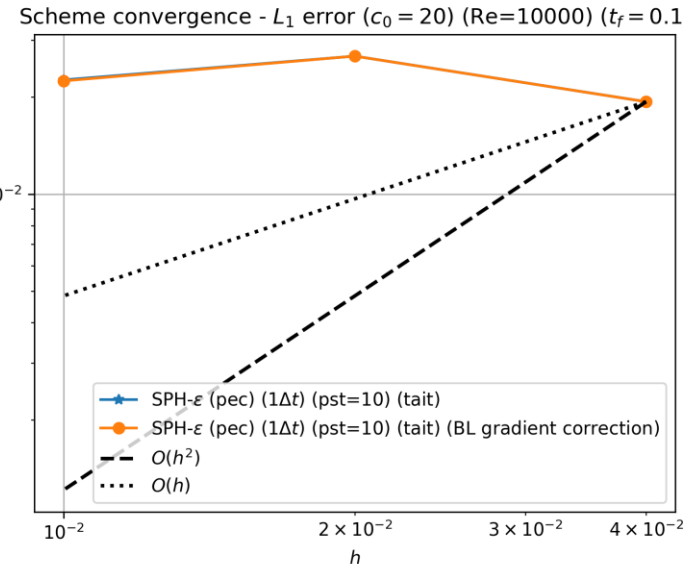


**Fig:** Convergence of the SPH- $\epsilon$  scheme without and with gradient correction ( $Re = 10^4$ )

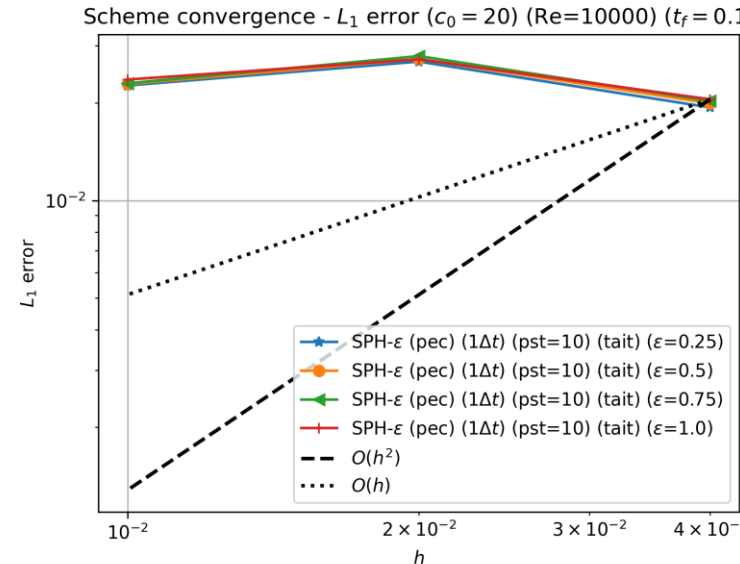


**Fig:** Convergence of the SPH- $\epsilon$  scheme for various values of  $\epsilon$  ( $Re = 10^4$ )

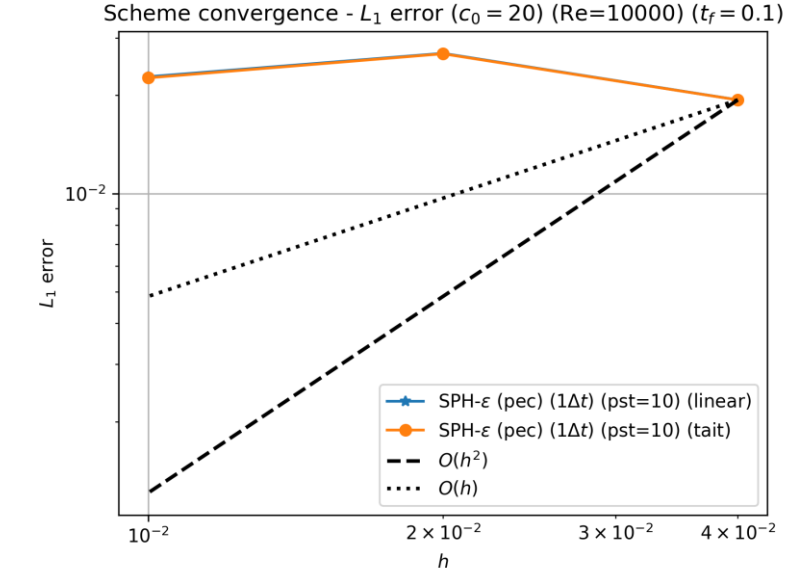


**Fig:** Convergence of the SPH- $\epsilon$  scheme for various equations of state ( $Re = 10^4$ )

## Observations

- Gradient correction: No effect on the OOC, accuracy, velocity field or energy spectrum of the scheme
- EOS: No effect on the OOC, accuracy, velocity field or energy spectrum of the scheme
- $\epsilon$ : No effect on the OOC or accuracy of the scheme; Increased  $\epsilon \rightarrow$  More diffused velocity field
- $f_{pst}$ :
  - Larger values  $\rightarrow$  Reduced magnitude of  $L_1$  error but no apparent effect on OOC
  - Larger values/No PST  $\rightarrow$  Clustering of particles; Domain is no longer uniform

# Long-time Simulation - Taylor-Green Vortex Problem

- Optimised SPH schemes documented
- Long-time test-case
  - TGV problem ( $t_f = 2$ ):  $Re = [10^4, 10^5]$ ;  $N = [100^2, 200^2]$

Turbulence Model	Scheme Name	PST Frequency	Equation of State	Integrator	CFL	Scheme-specific Parameters	Time Taken (s) ( $N = 200^2, Re = 10^5$ )
Viscosity – based <i>(Standard Lagrangian)</i>	Lagrangian with iterative PST and coupled_c viscosity formulation <b>(L-IPST-C)</b>	10	TaitEOS	PEC	1	---	5900
LES – based <i>(Explicit P-EOS)</i>	<b>SPH-LES</b>	10	TaitEOS	PEC	1	Viscous models=[SMAG, SMAG-MCG, SIGMA];	---
Lagrangian-LES – based	<b><math>\delta</math>-LES-SPH</b>	10	TaitEOS	RK2	1.5	No gradient correction;	8200
RANS – based	<b><math>k - \epsilon</math> SPH</b>	10	TaitEOS	PEC	1	Simplified $k - \epsilon$ transport equations;	6400
LANS - based	<b>SPH-<math>\epsilon</math></b>	10	TaitEOS	PEC	1	No gradient correction; $\epsilon=0.5$ ;	3000

# Long-time TGV Analysis

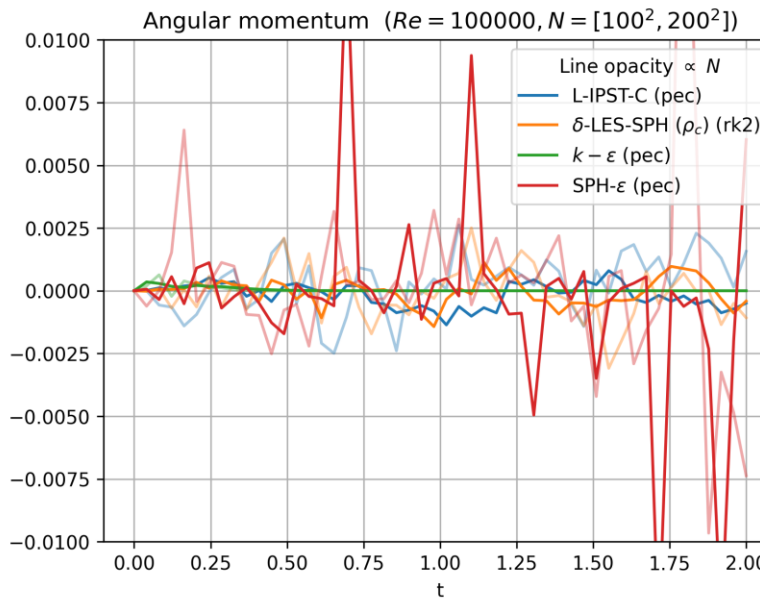


**Fig:** Evolution of the angular momentum for various schemes ( $Re = 10^5$ ) (zoomed in)

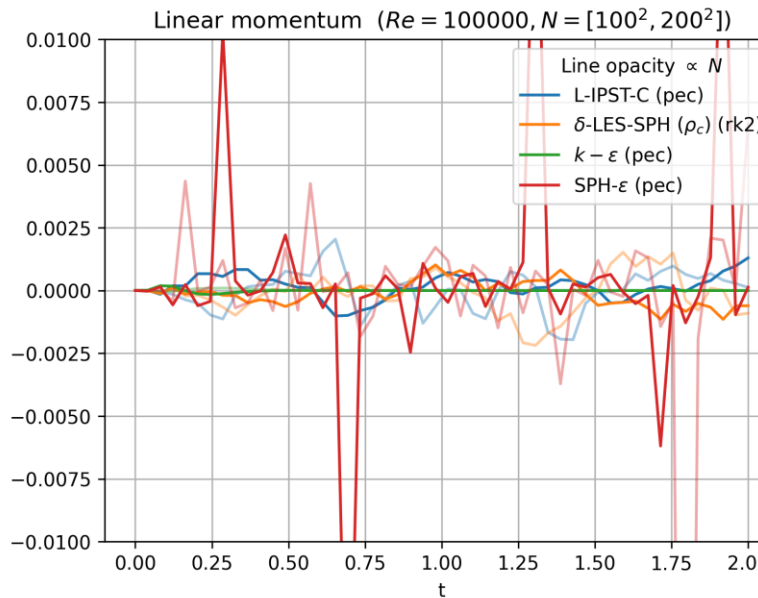


**Fig:** Evolution of the linear momentum for various schemes ( $Re = 10^5$ ) (zoomed in)

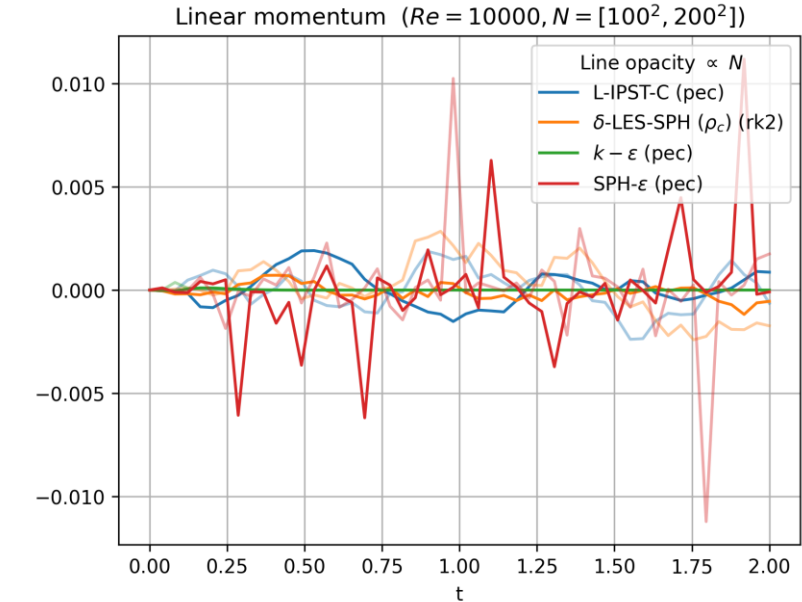


**Fig:** Evolution of the linear momentum for various schemes ( $Re = 10^5$ )

## Observations

- No external forces  $\rightarrow$  Angular & linear momentum should be **conserved**
- L-IPST-C &  $\delta$ -LES-SPH :
  - Oscillate about zero
  - Stay bounded; Increased resolution  $\rightarrow$  bounds decrease
- $k - \epsilon$  SPH : Almost perfectly conservative
- SPH- $\epsilon$  :
  - Arbitrary jumps in the momentum plots  $\rightarrow$  Not conservative
  - Increased resolution  $\rightarrow$  No convergence

# Long-time TGV Analysis

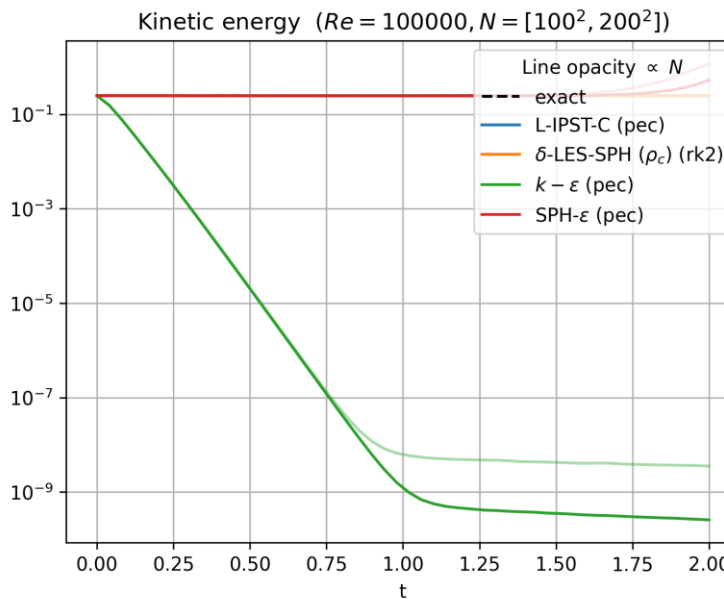


**Fig:** Evolution of the kinetic energy for various schemes ( $Re = 10^5$ )

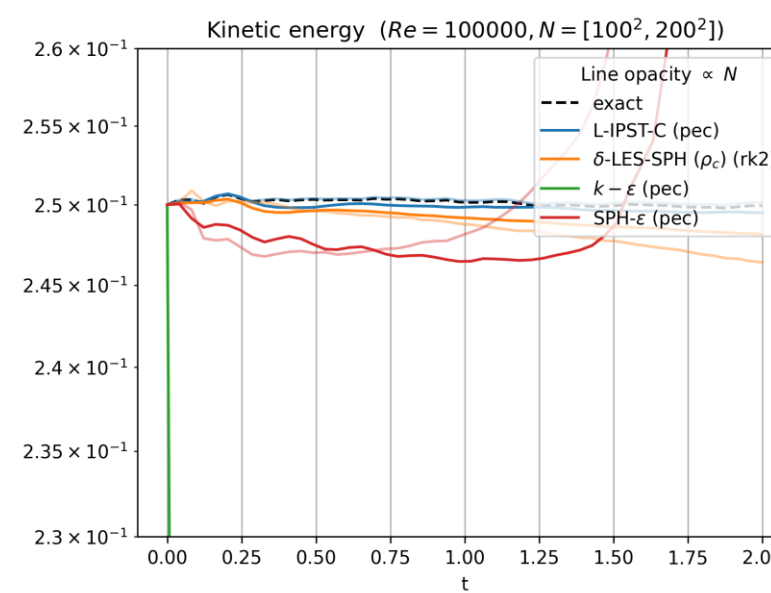


**Fig:** Evolution of the kinetic energy for various schemes ( $Re = 10^5$ ) (zoomed in)

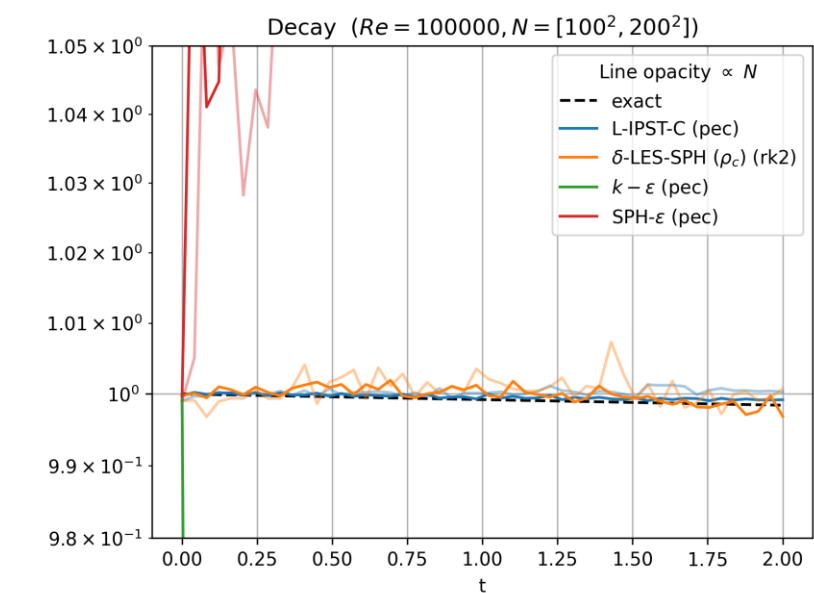


**Fig:** Evolution of the velocity decay for various schemes ( $Re = 10^5$ ) (zoomed in)

## Observations

- L-IPST-C &  $\delta$ -LES-SPH :
  - Track exact solution accurately
  - Increased resolution → Increased accuracy
- $k - \epsilon$  SPH : Dissipates all the energy → **Non-physical** solution
- SPH- $\epsilon$  : Adds energy to the system → System diverges

# Long-time TGV Analysis

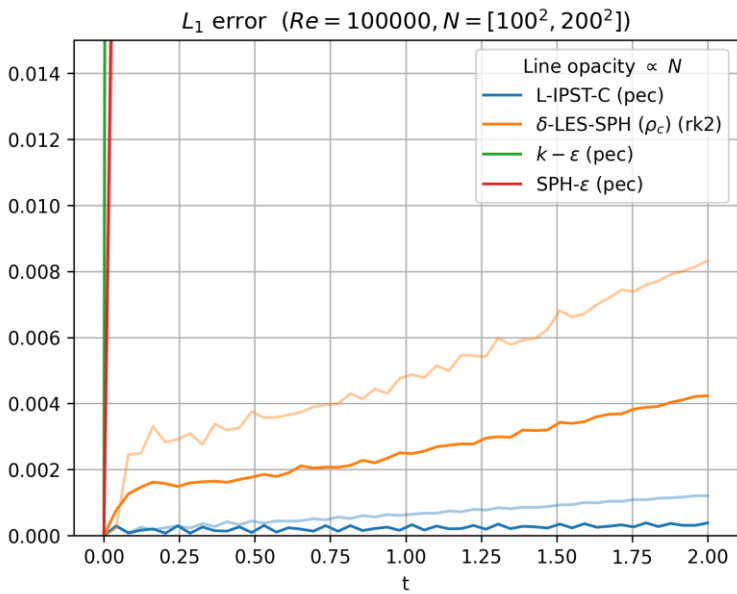


**Fig:** Evolution of the  $L_1$  error for various schemes ( $Re = 10^5$ )

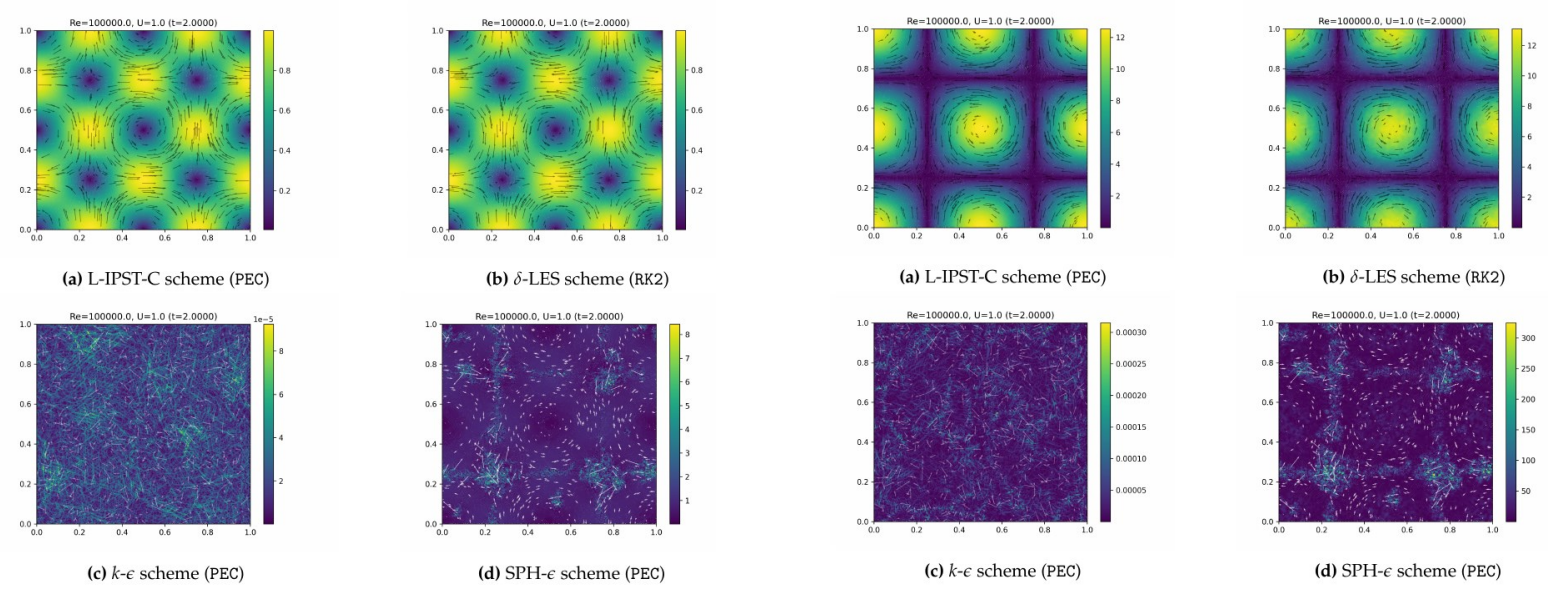


**Fig:** Velocity magnitude field (arrows represent the velocity vector) for various schemes ( $Re = 10^5$ )

**Fig:** Vorticity magnitude field (arrows represent the velocity vector) for various schemes ( $Re = 10^5$ )

## Observations

- L-IPST-C &  $\delta$ -LES-SPH :
  - Have relatively the least amount of error
  - Capture both the velocity and vorticity field accurately
- $k - \epsilon$  SPH : Drains all the energy from the system; No structure in the flow field
- SPH- $\epsilon$  :
  - High magnitude of  $L_1$  error
  - TGV structures present in the flow field, albeit with the magnitude blown-up
  - Addition of a dissipative mechanism → Might improve performance

# Long-time TGV Analysis

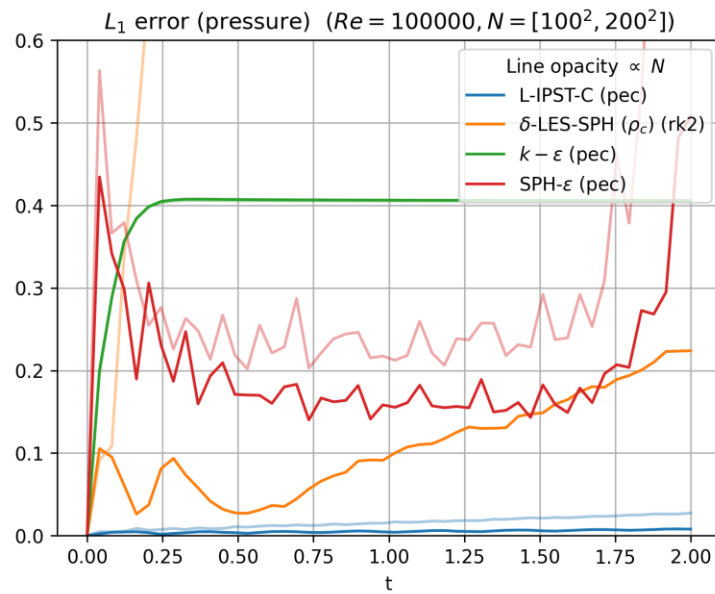


**Fig:** Evolution of the  $L_1$  error (pressure) for various schemes ( $Re = 10^5$ )

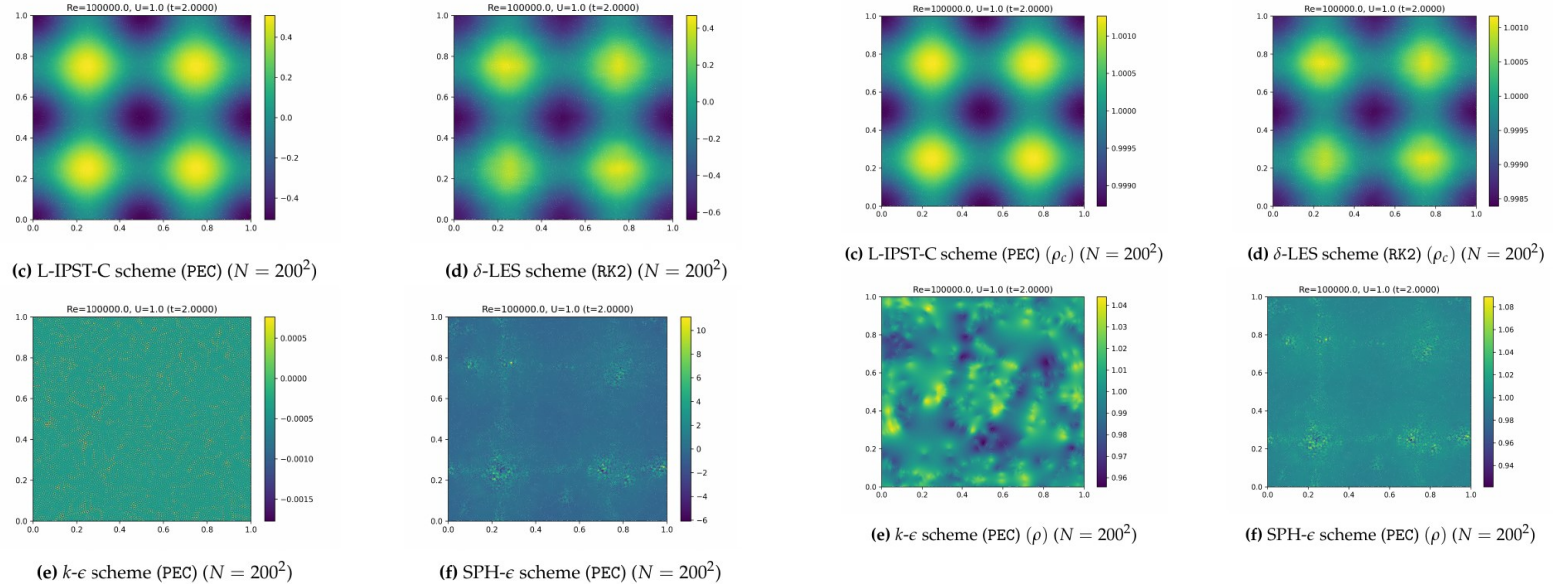


**Fig:** Pressure magnitude field (arrows represent the velocity vector) for various schemes ( $Re = 10^5$ )

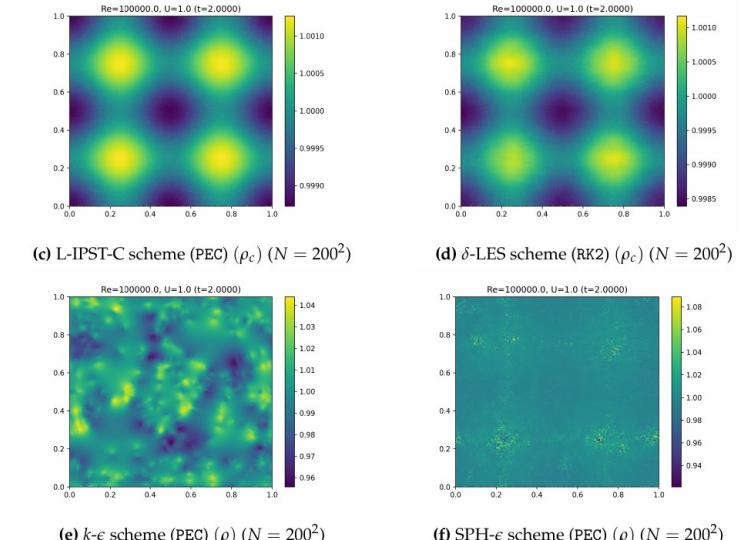


**Fig:** Density magnitude field (arrows represent the velocity vector) for various schemes ( $Re = 10^5$ )

## Observations

- L-IPST-C: Least amount of error; Reduces with resolution
- $\delta$ -LES-SPH:
  - Significantly **dependent** on the resolution
  - Trends in density & pressure field are captured well, but the limits are larger
- $k - \epsilon$  SPH : Non-existent and noisy density & pressure fields
- SPH- $\epsilon$  :
  - Comparable error to  $\delta$ -LES-SPH, and similar (but exaggerated) cause as well

# Long-time TGV Analysis

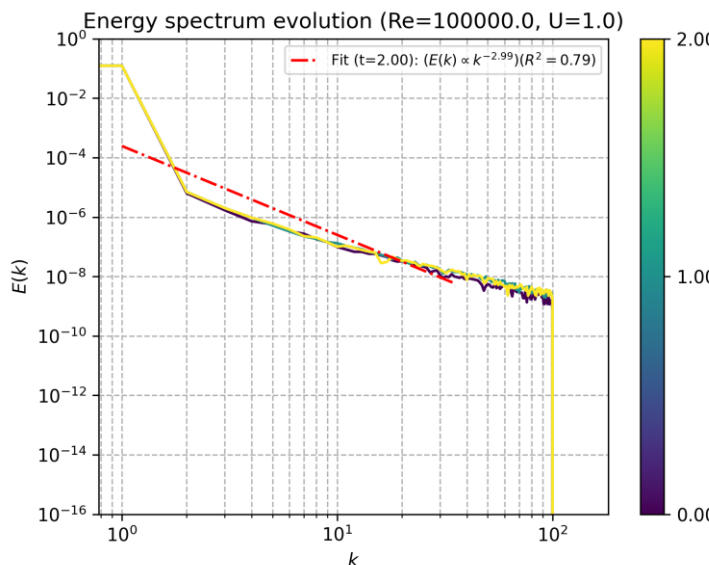


**Fig:** Evolution of the energy spectrum (L-IPST-C) ( $Re = 10^5, N = 200^2$ )

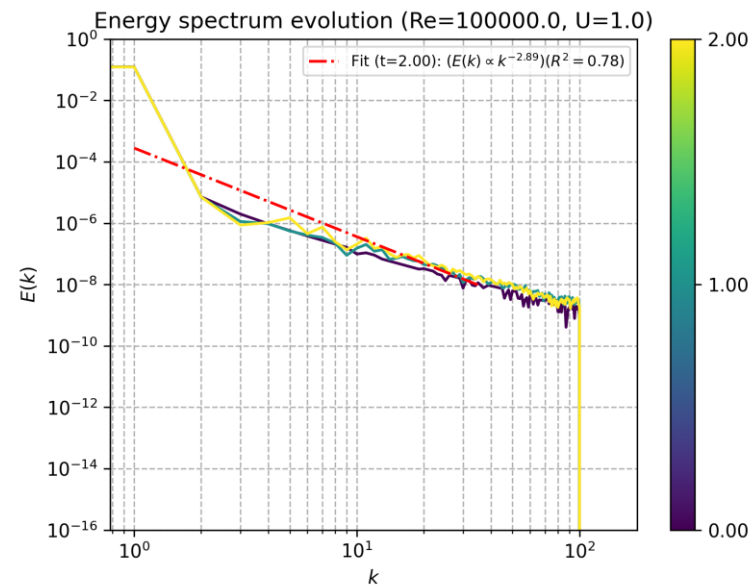


**Fig:** Evolution of the energy spectrum ( $\delta$ -LES-SPH) ( $Re = 10^5, N = 200^2$ )

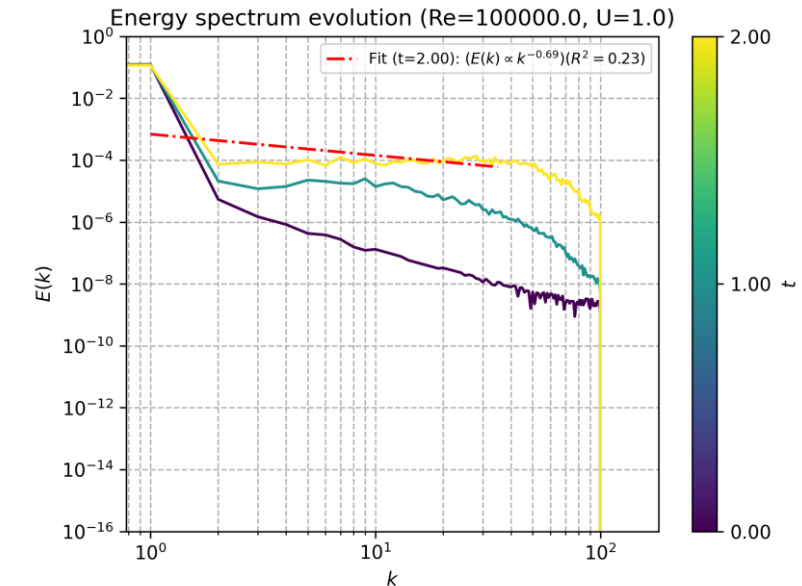


**Fig:** Evolution of the energy spectrum (SPH- $\epsilon$ ) ( $Re = 10^5, N = 200^2$ )

## Observations

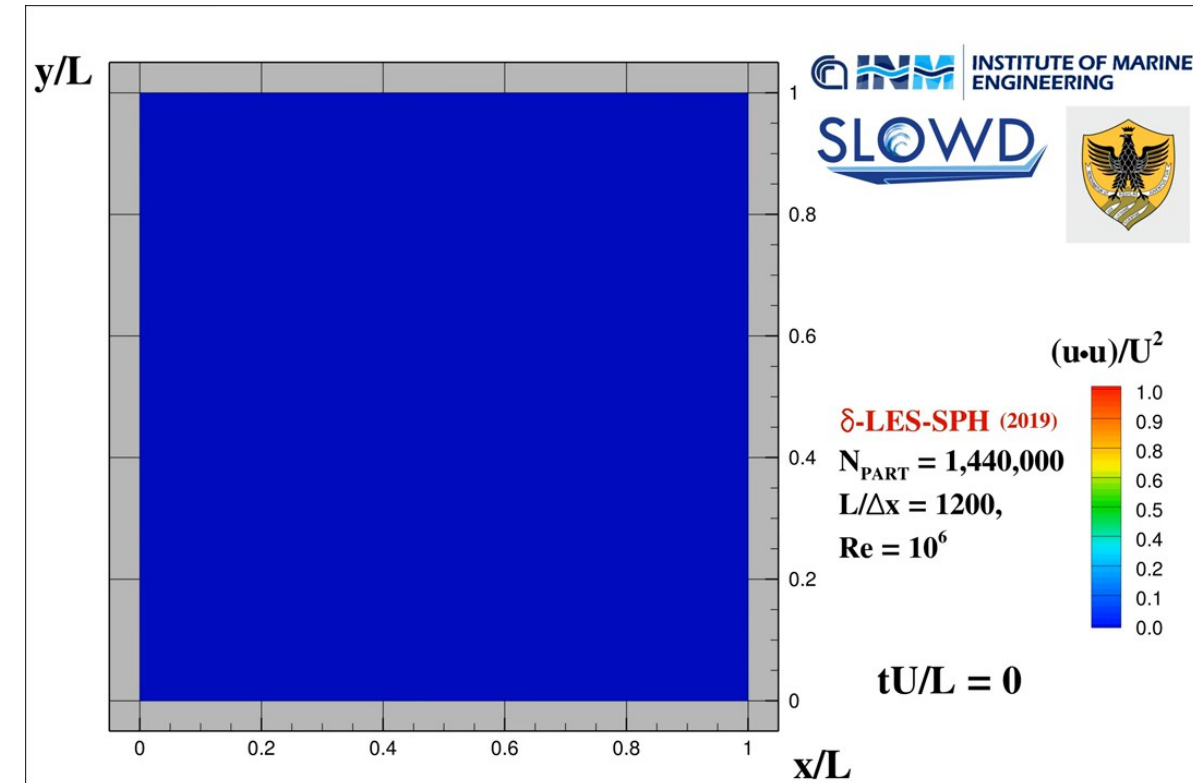
- L-IPST-C &  $\delta$ -LES-SPH :
  - Similar energy dissipation over time
  - $\delta$ -LES-SPH → slightly better at **redistributing** energy to smaller scales
- $k - \epsilon$  SPH : Dissipates energy at all scales
- SPH- $\epsilon$  : Increases energy to the smaller scales; negligible effect on larger scales

# Externally Forced Variant - Taylor-Green Vortex Problem

- Perform unsteady analysis on L-IPST-C &  $\delta$ -LES-SPH schemes
- Externally forced TGV simulated based on the work of Antuono et al. 2021
- Reference simulation parameters
  - $Re = [10^4, 10^5, 10^6]$ ;  $N = 1200^2$ ;  $t_f = 20$
- Simulation parameters
  - $Re = [10^4, 10^5, 10^6]$ ;  $N = [100^2, 200^2]$ ;  $t_f = 3$

$$\mathbf{F}_{2D} = r(t^*) A \left( \sin(8\pi x^*) \cos(8\pi y^*), -\cos(8\pi x^*) \sin(8\pi y^*) \right)$$

$$r(t^*) = \begin{cases} 10t^* & \text{for } t^* \in [0, 0.1) \\ 1 & \text{for } t^* \in [0.1, 0.9) \\ 10(1 - t^*) & \text{for } t^* \in [0.9, 1) \\ 0 & \text{for } t^* \geq 1 \end{cases}$$



**Vid:** [SPH LES TurboMixer N1200 Re=1M, Q, Curl, Pr, Lyap.](#) (Rep: Antuono2021)

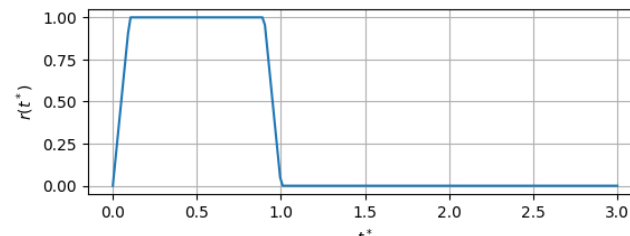


**Fig:** Ramp function

[1] M. Antuono, S. Marrone, A. Di Mascio, and A. Colagrossi, "Smoothed particle hydrodynamics method from a large eddy simulation perspective. Generalization to a quasi-Lagrangian model," Phys. Fluids, vol. 33, no. 1, p. 015102, Jan. 2021, doi: 10.1063/5.0034568.

# Externally Forced TGV Analysis

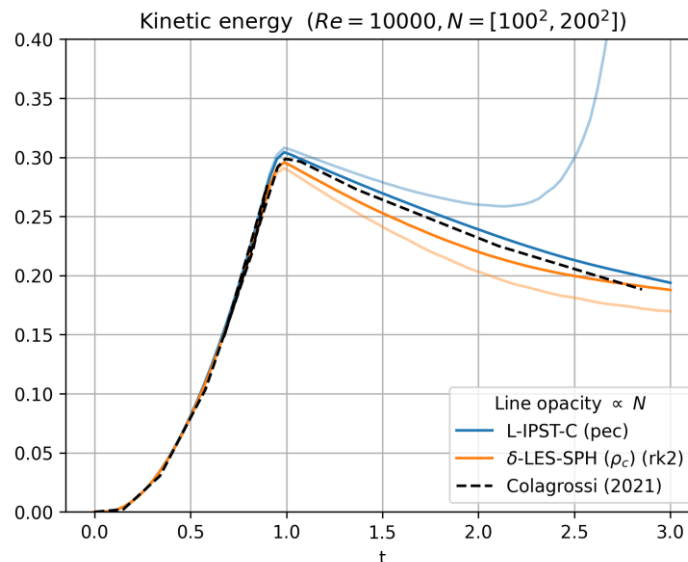


**Fig:** Evolution of the kinetic energy ( $Re = 10^4$ )

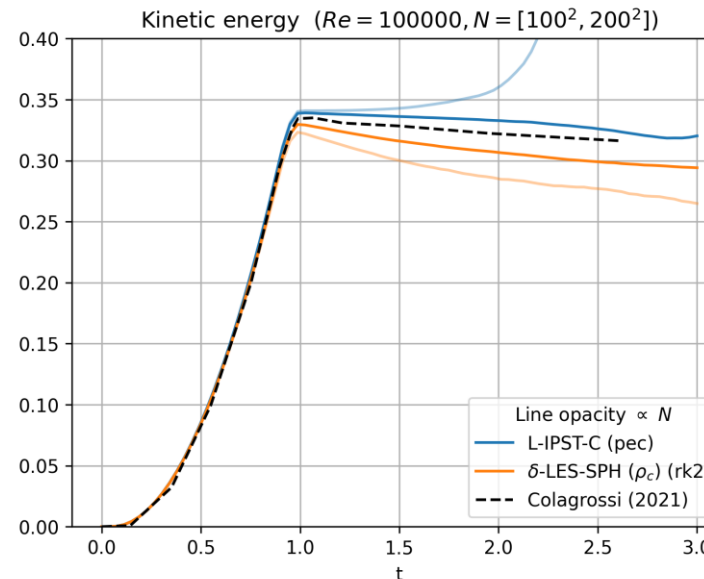


**Fig:** Evolution of the kinetic energy ( $Re = 10^5$ )

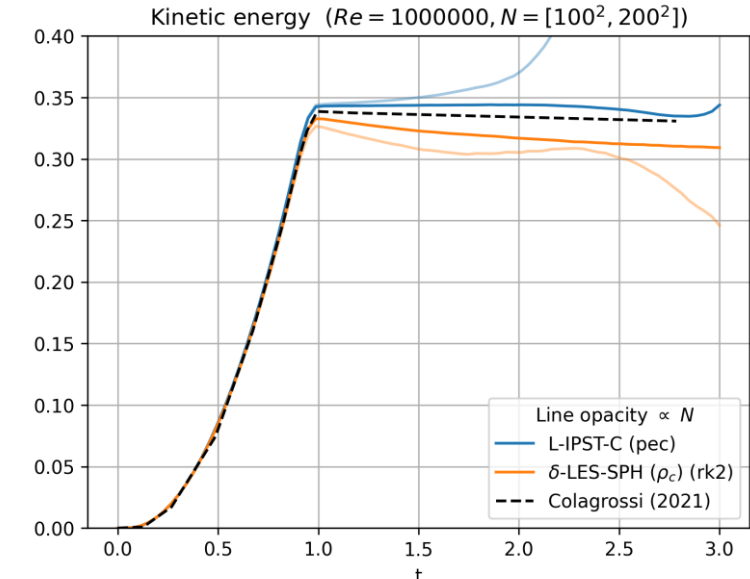


**Fig:** Evolution of the kinetic energy ( $Re = 10^6$ )

## Observations

- L-IPST-C :
  - Blows up for  $N = 100^2$ ; Increased resolution → Tracks reference well
  - Over-predicts the reference → Cause for solution diverging
- $\delta$ -LES-SPH :
  - Under-predicts the reference → Improves with increased resolution
- In the limit  $h \rightarrow 0$  both the schemes appear to converge to the reference

# Externally Forced TGV Analysis

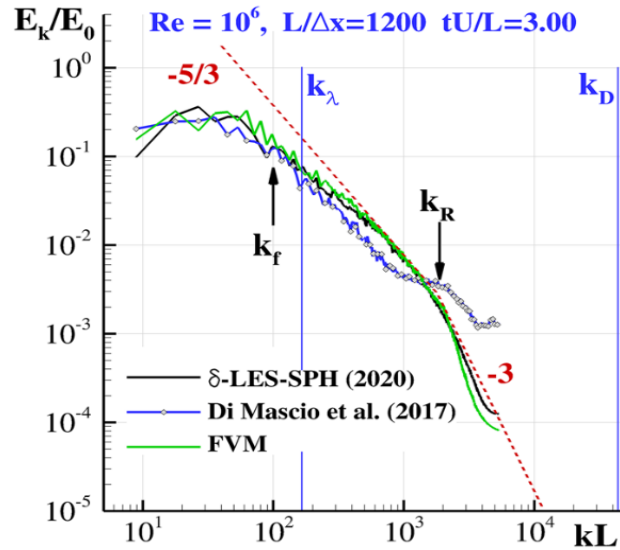


**Fig:** Evolution of the energy spectrum ( $Re = 10^6$ ). (Rep: Antuono2021)

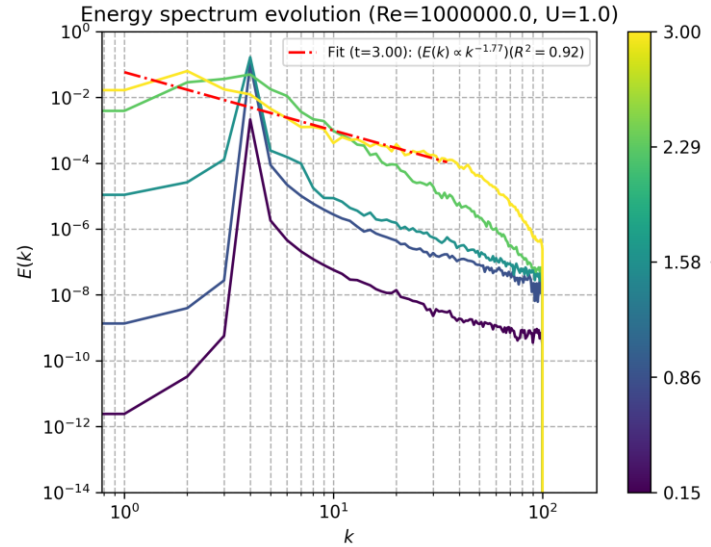


**Fig:** Evolution of the energy spectrum ( $Re = 10^6$ ) (L-IPST-C)

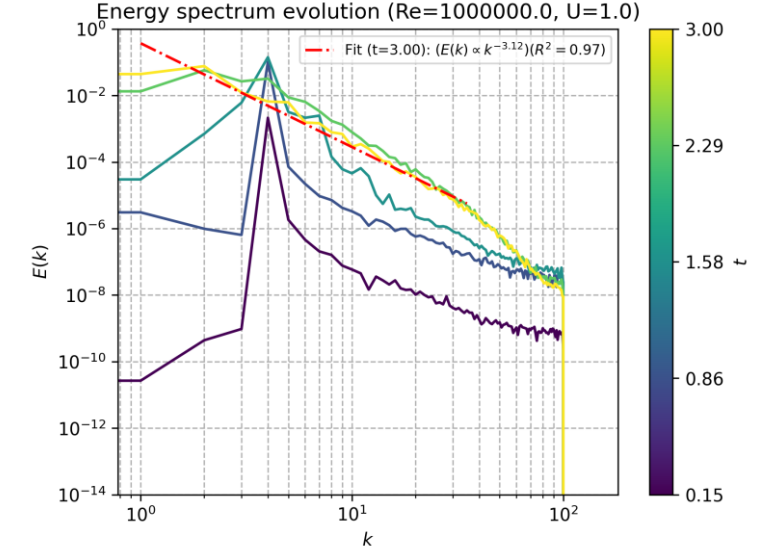


**Fig:** Evolution of the energy spectrum ( $Re = 10^6$ ) ( $\delta\text{-LES-SPH}$ )

## Observations

- L-IPST-C :
  - Inertial sub-range  $\rightarrow$  Slope at ( $t_f = 3$ ) =  $-1.77 \approx -5/3$
  - Viscous sub-range  $\rightarrow$  Slope at ( $t_f = 3$ )  $\in (-3, -2)$  (Affected – lower slope)
  - Viscous dissipation mechanism  $\rightarrow$  Not strong enough at smaller scales
    - Either increase resolution or requires a sub-grid scale model
- $\delta\text{-LES-SPH}$  :
  - Inertial sub-range  $\rightarrow$  Slope at ( $t_f = 3$ ) =  $-3.12$  (Affected – higher slope)
  - Viscous sub-range  $\rightarrow$  Slope at ( $t_f = 3$ )  $\in (-4, -3.2)$
  - Viscous dissipation mechanism  $\rightarrow$  Overly-powerful at smaller scales; Needs to be tuned

# Externally Forced TGV Analysis

$tU/L = 3.00$        $L/\Delta x = 1200$ ,  $Re = 10^6$

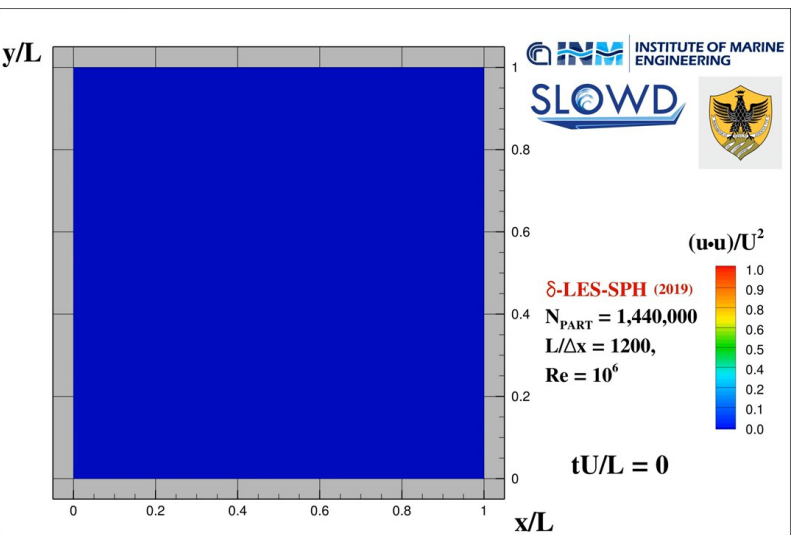
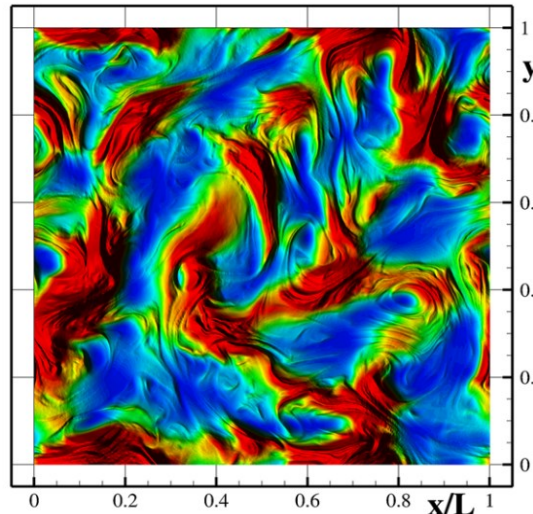


**Fig:** Velocity magnitude field at  $t_f = 3$  ( $Re = 10^6$ ). (Rep: Antuono2021)

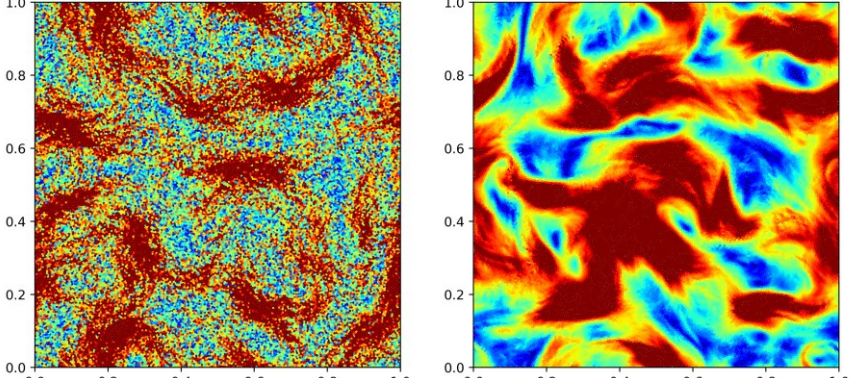
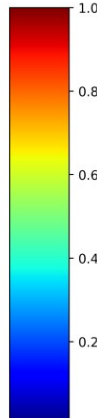
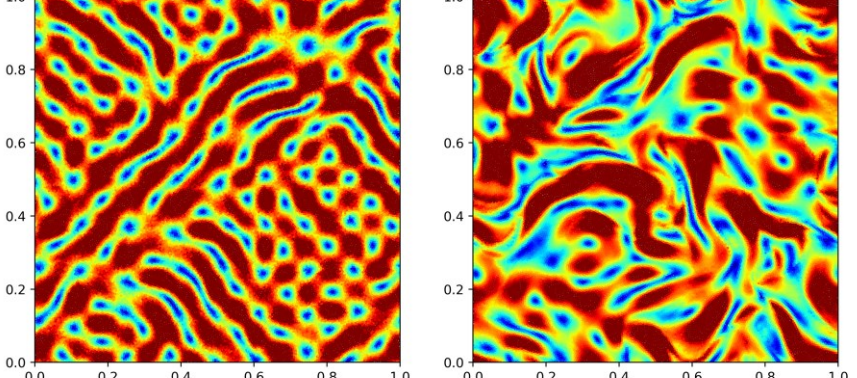
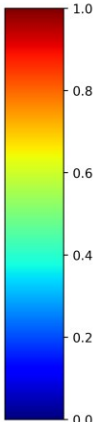
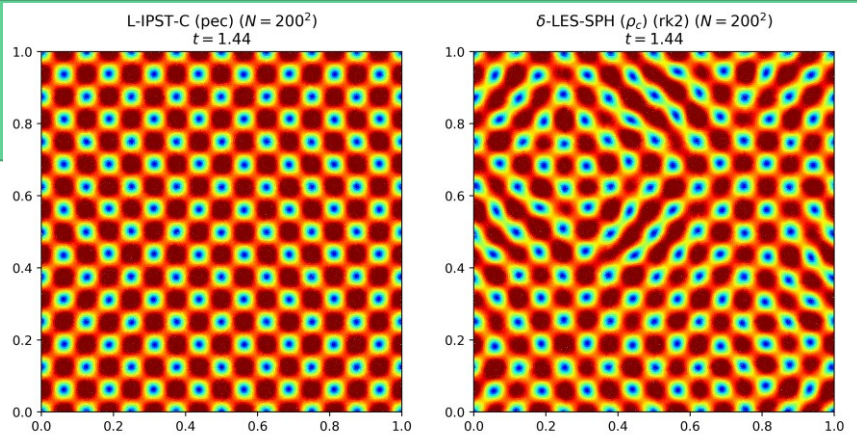


**Fig:** Velocity magnitude field computed at  $t_f = [1, 1.94, 3]$  ( $Re = 28 \times 10^6$ )

## Observations

- L-IPST-C :
  - Maintains the field trends along with magnitude till  $t_f = 1.9$
  - Smaller scales → Energetic particles move freely throughout the domain without forming **localised eddies**
- $\delta$ -LES-SPH :
  - Maintains the field trends along with magnitude (under-predicted) throughout → Velocity field diffuses earlier
  - **Large** distinct zones of high velocity formed
  - Zones of low velocity is **sparse** compared to reference

# Externally Forced TGV Analysis

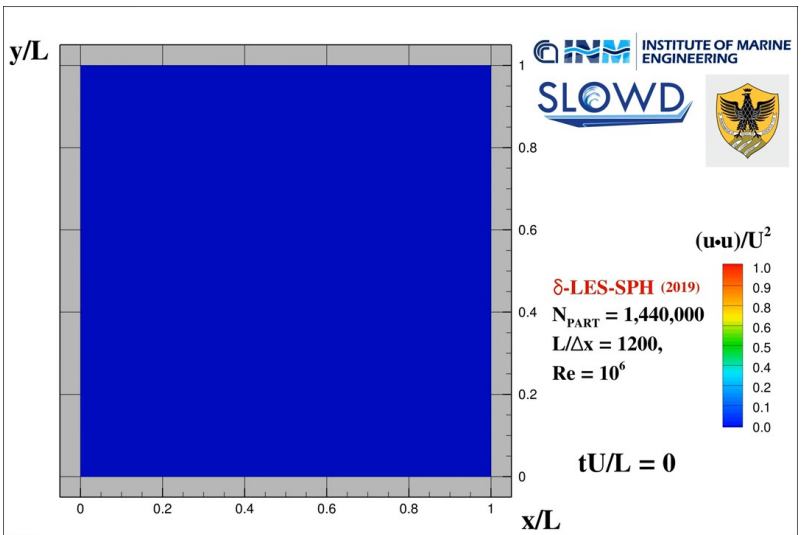
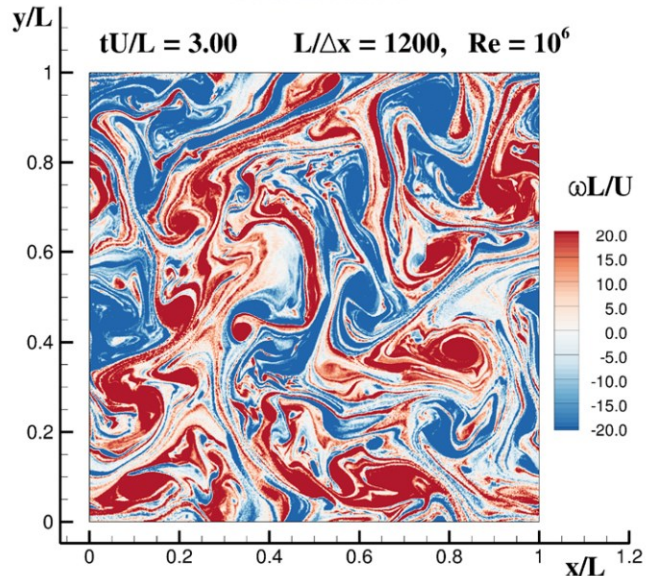


**Fig:**  $\omega_z$  field at  $t_f = 3$  ( $Re = 10^6$ ). (Rep: Antuono2021)

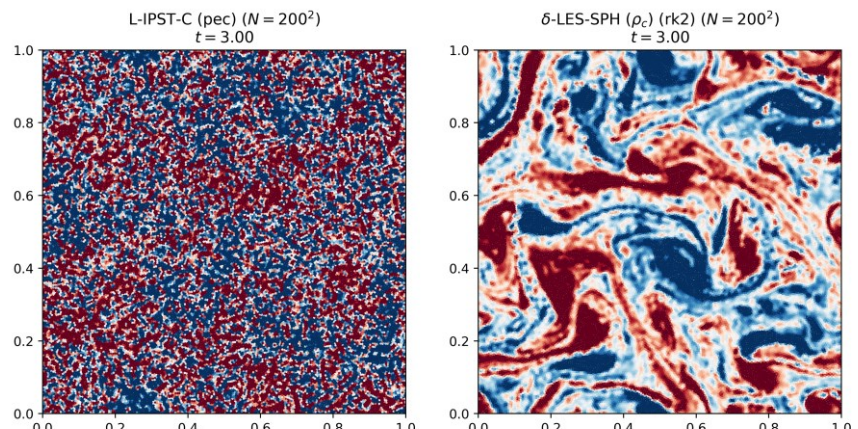
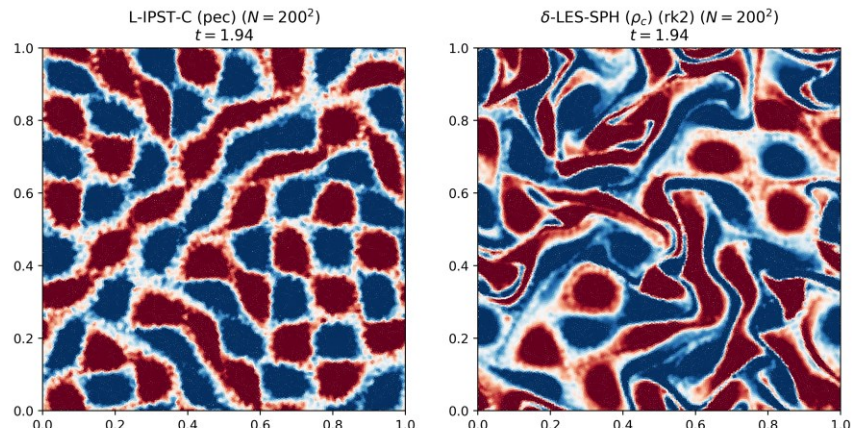
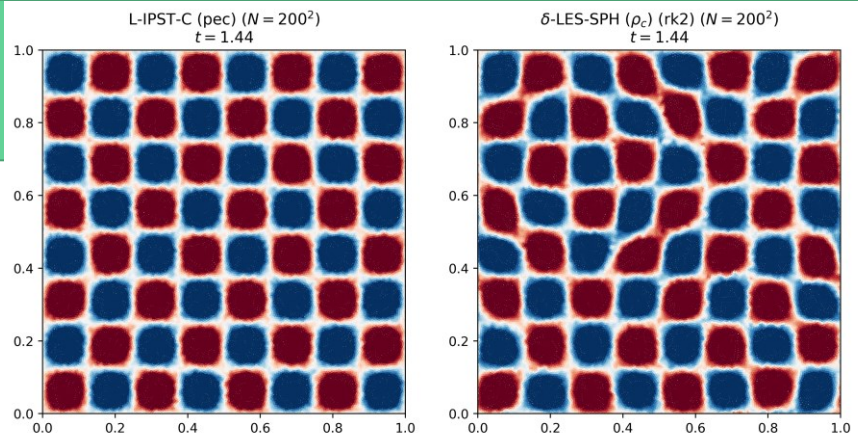


**Fig:**  $\omega_z$  field computed at  $t_f = [1, 1.94, 3]$  ( $Re = 10^6$ )

## Observations

- L-IPST-C :
  - Maintains the field trends along with magnitude till  $t_f = 2$
  - Loses all structural information subsequently, and turns into a **noisy field**
- $\delta\text{-LES-SPH}$  :
  - Maintains the field trends along with magnitude till  $t_f = 1.8$
  - Diffusion of vorticity begins **earlier**
  - Final flow field contains **fewer & larger** eddies

# Externally Forced TGV Analysis

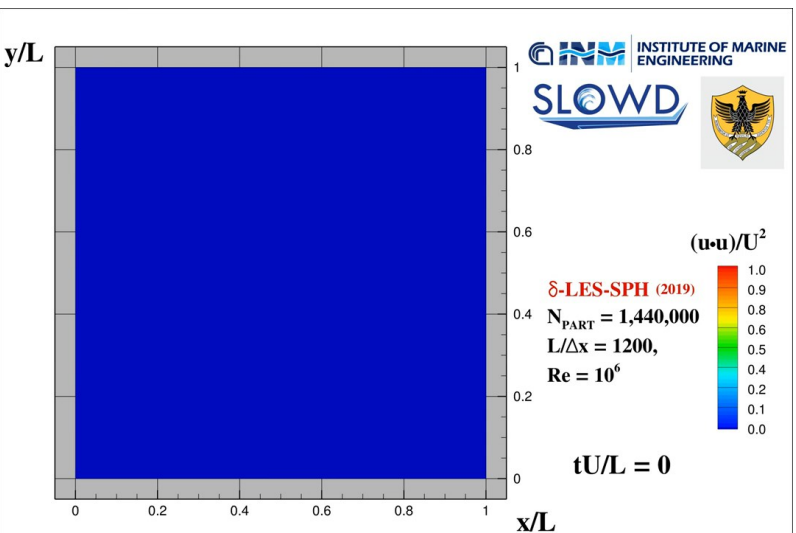
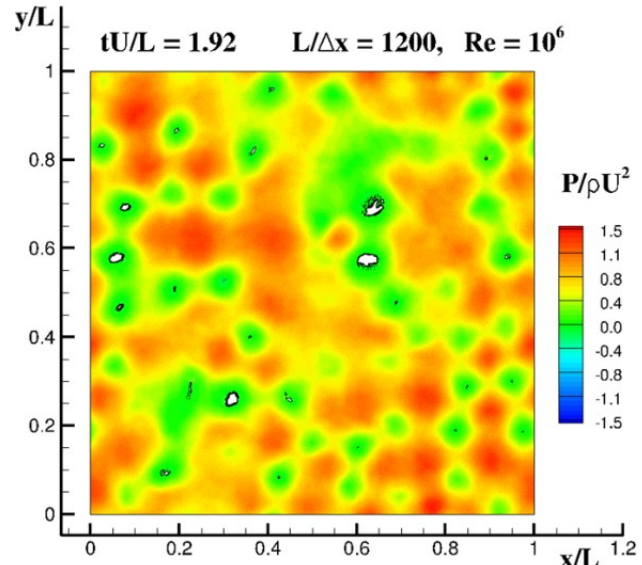


**Fig:** Pressure field at  $t_f = 3$  ( $Re = 10^6$ ). (Rep: Antuono2021)

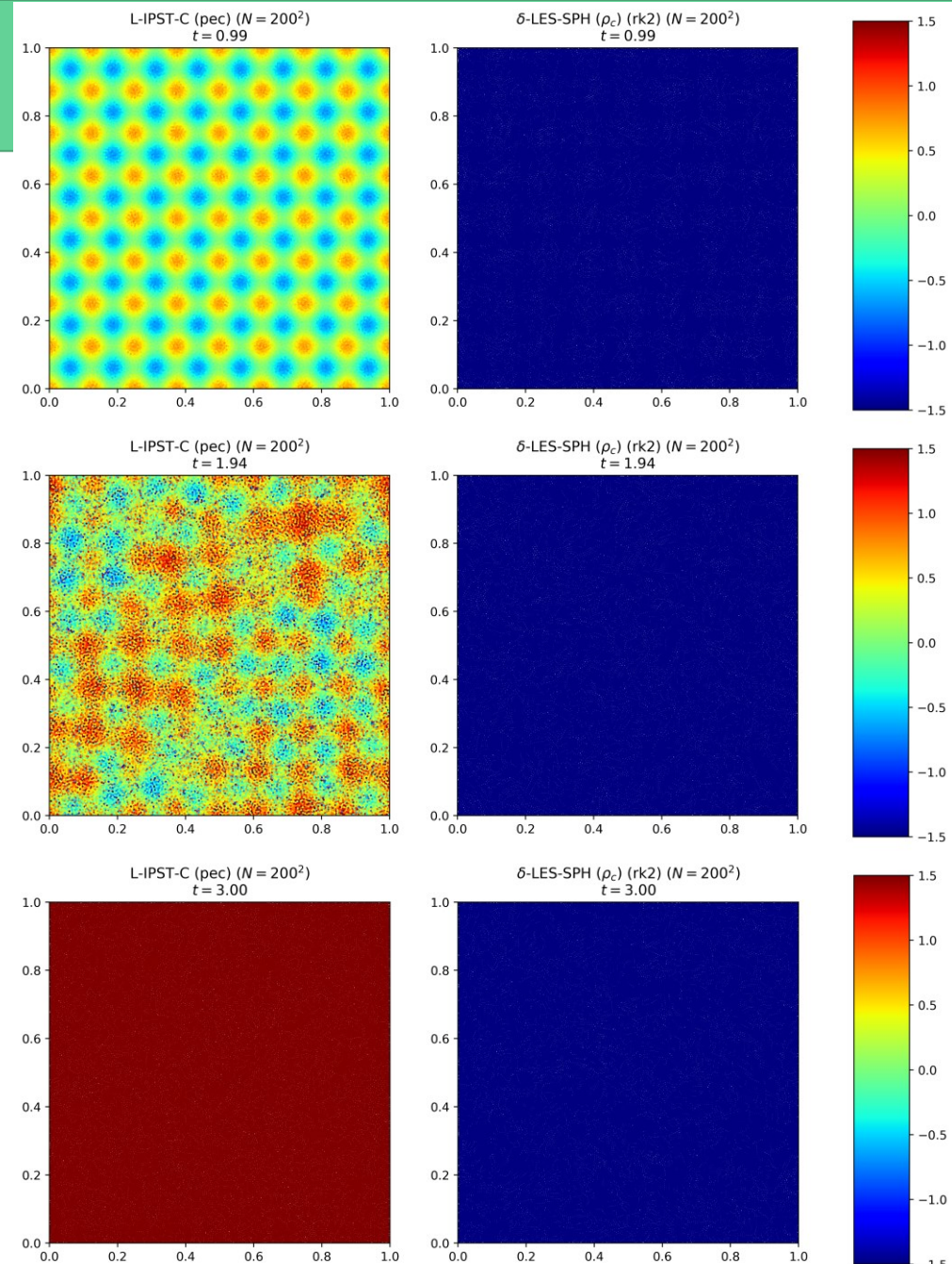


**Fig:** Pressure field computed at  $t_f = [1, 1.94, 3]$  ( $Re = 10^6$ )

## Observations

- L-IPST-C :
  - Maintains the field trends
- $\delta$ -LES-SPH :
  - Limits are much lower, but trends are maintained till  $t_f = 1.92$

# Externally Forced TGV Analysis

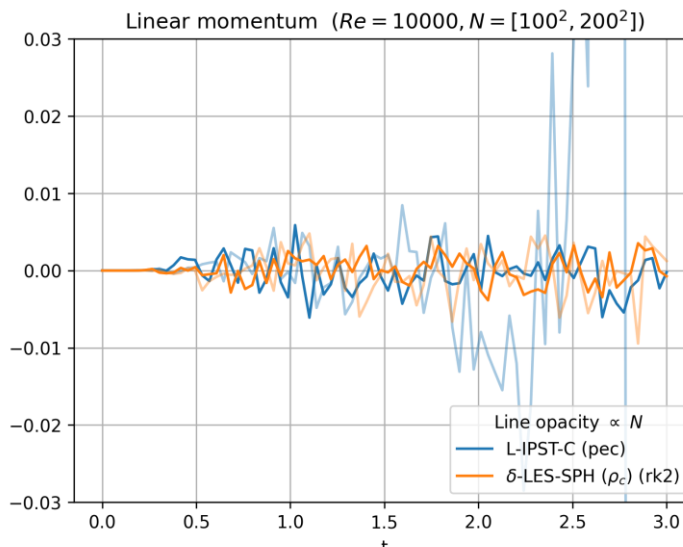


**Fig:** Evolution of the linear momentum ( $Re = 10^4$ ) (zoomed in)

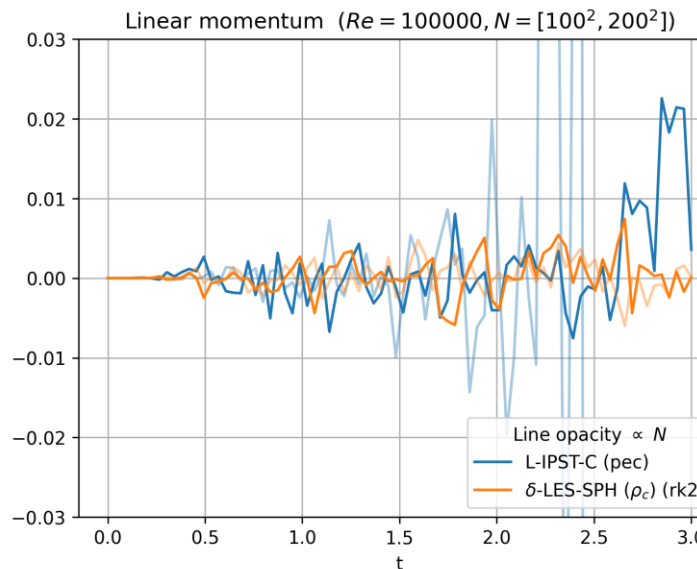


**Fig:** Evolution of the linear momentum ( $Re = 10^5$ ) (zoomed in)

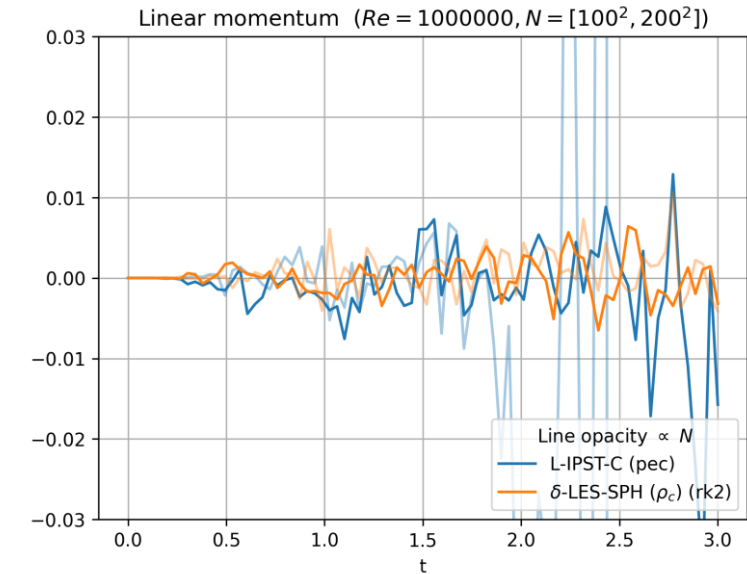


**Fig:** Evolution of the linear momentum ( $Re = 10^6$ ) (zoomed in)

## Observations

- Net force acting on the system is zero → Therefore momentum must be conserved
- L-IPST-C :
  - Accuracy increases with increased resolution
  - Noticeable peaks are still found at high  $Re$  even for large  $N$
- δ-LES-SPH :
  - Graphs are much closer to the zero line
  - No arbitrary peaks in the plot → Much more conservative than L-IPST-C at high  $Re$

# Conclusion

- Comprehensive **database** of past SPH turbulence models
  - Including their SPH discretisations, limitations & areas for refinement
- Better understanding of turbulence-specific post-processing techniques in SPH
- Developed **TurbulentFlowApp**, which can be incorporated into PySPH : Post-processing related helper class
- Identified five representative SPH schemes from each of the major turbulence model category
- Performed OOC analysis on said schemes, and optimised the scheme-specific parameters to improve their performance
- The accompanying code for these schemes can be made open-source to enhance the **reproducibility** of the work
- Performed long-time TGV simulations, to study the evolution of the flow-variables & scheme instability
  - Demonstrated **instability** in SPH- $\epsilon$  &  $k - \epsilon$  SPH schemes, at least for the unbounded problem
  - Demonstrated the **promising** results of L-IPST-C &  $\delta$ -LES-SPH schemes
  - Identified areas of refinement for all the schemes in consideration
- L-IPST-C &  $\delta$ -LES-SPH scheme using the externally-forced TGV problem
  - Identified potential ways to improve these schemes based on their key characteristics & issues

# Future Work

- Attempt to combine the **compressible** EDAC scheme with Lagrangian-LES filtering
- Robust methods of tracking LCSs need to be studied and implemented
- Identified the inadequacy of TGV as a benchmark problem for turbulence specifically
  - Future work involving problems with boundaries will be necessary to evaluate the schemes in a realistic setting
- Implement a faster & efficient variant of the **periodic** boundary conditions to run problems of much finer resolution in a reasonable time
- Incorporate boundary conditions & wall functions to solve real-world problems
- Incorporate adaptive refinement to reduce the computational load

# *Thank you!*



## ***Acknowledgements***

*I would like to acknowledge the mentorship of my guide, [Prof. Prabhu Ramachandran](#), and the members of his lab group for their inputs and support.*

*I also appreciate the research environment provided by the [Indian Institute of Technology Bombay](#), and particularly, the [Department of Aerospace Engineering](#) for having given me this platform to pursue my graduate studies.*

*I am also thankful for the [professors on the panel](#) for their time today, and allowing me to present my work.*

Department of Aerospace Engineering  
Indian Institute of Technology Bombay

June 30<sup>th</sup>, 2023

# Appendix A

-- *Additional Results* --

# Large-Eddy Simulation-based Model (SPH-LES) Analysis

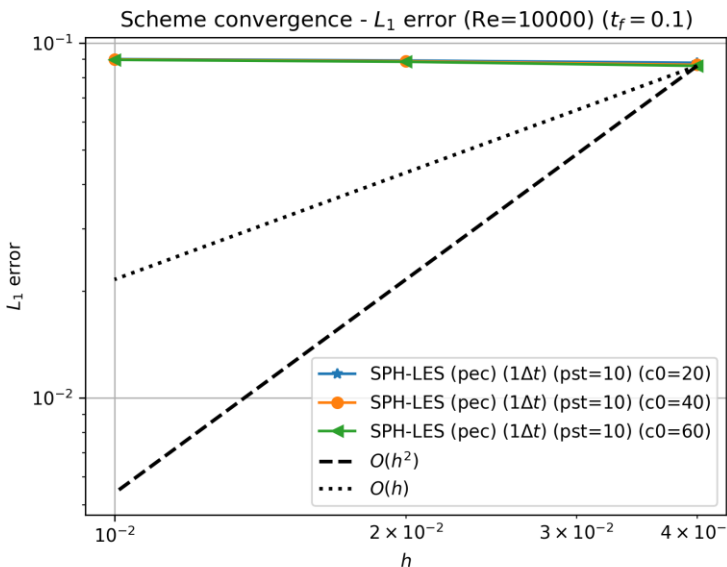


**Fig:** Convergence of the SPH-LES scheme for various speed of sound values ( $Re = 10^4$ )

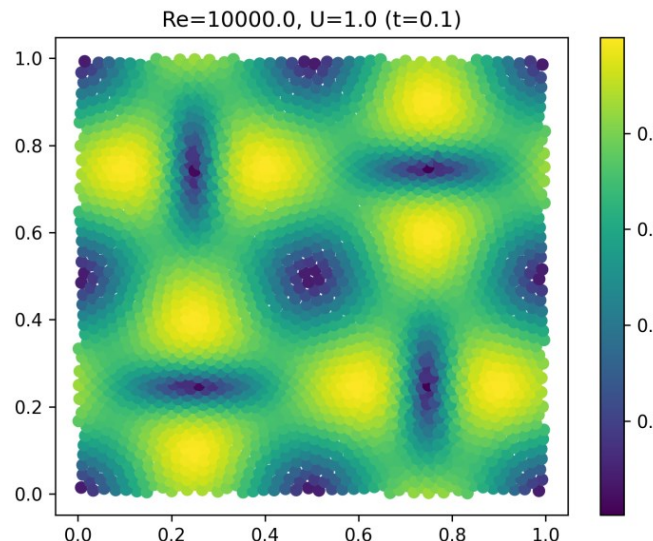


**Fig:** Velocity magnitude field for SPH-LES scheme ( $c_s = 20$ ) ( $Re = 10^4, N = 50^2$ )

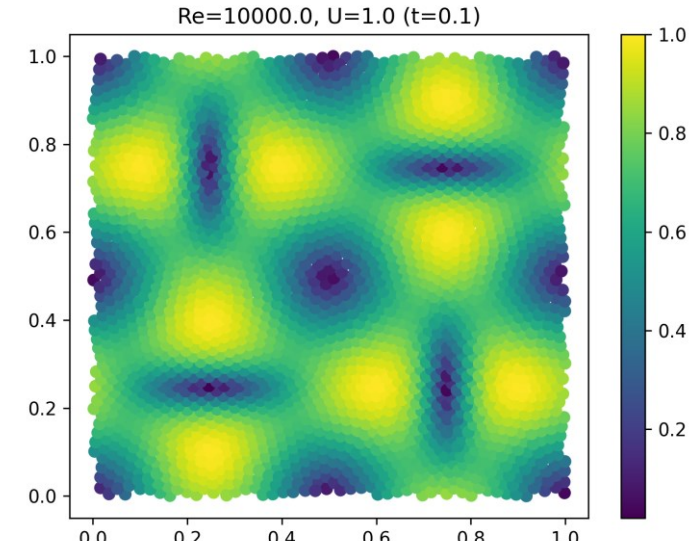


**Fig:** Velocity magnitude field for SPH-LES scheme ( $c_s = 60$ ) ( $Re = 10^4, N = 50^2$ )

## Observations

- $c_s$  : No effect on the SOC or accuracy
- Negligible difference in the distribution of the particles
- $c_s = 20$  chosen, based on run-time and accuracy trade-off

[Go back](#)

# Lagrangian LES-based Model ( $\delta$ -LES-SPH) Analysis

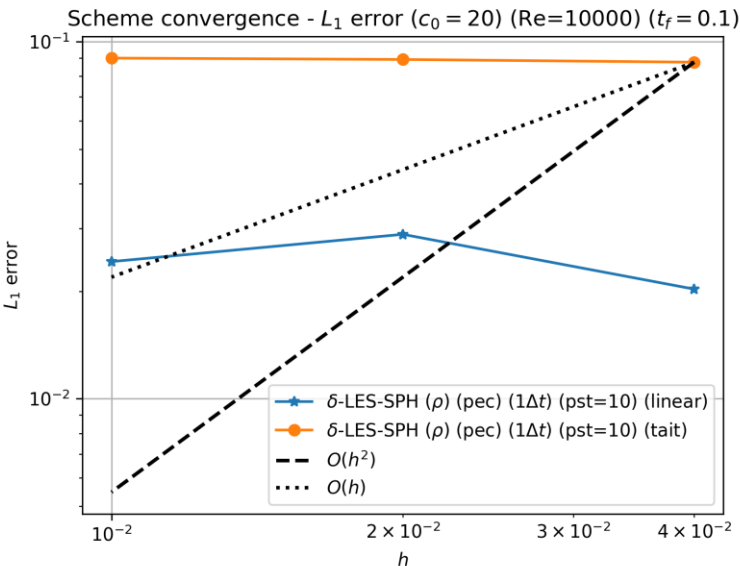


**Fig:** Convergence of the  $\delta$ -LES-SPH ( $\rho$ ) scheme for various equations of state ( $Re = 10^4$ )

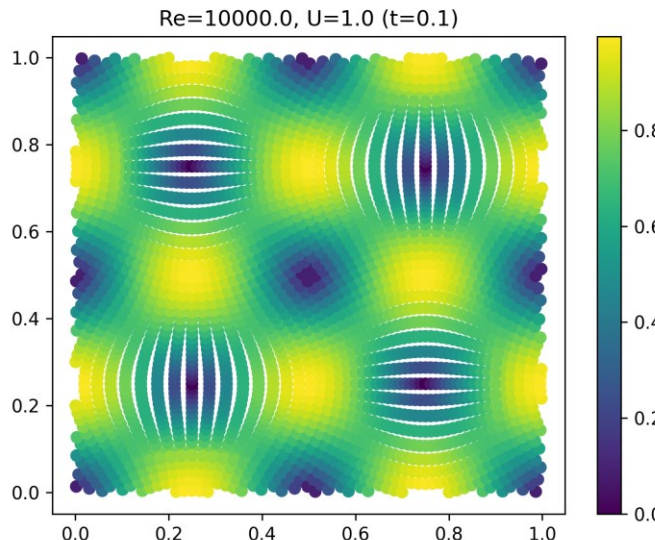


**Fig:** Velocity magnitude field for  $\delta$ -LES-SPH ( $\rho_c$ ) scheme ( $f_{pst} = \text{None}$ ) ( $Re = 10^4, N = 50^2$ )

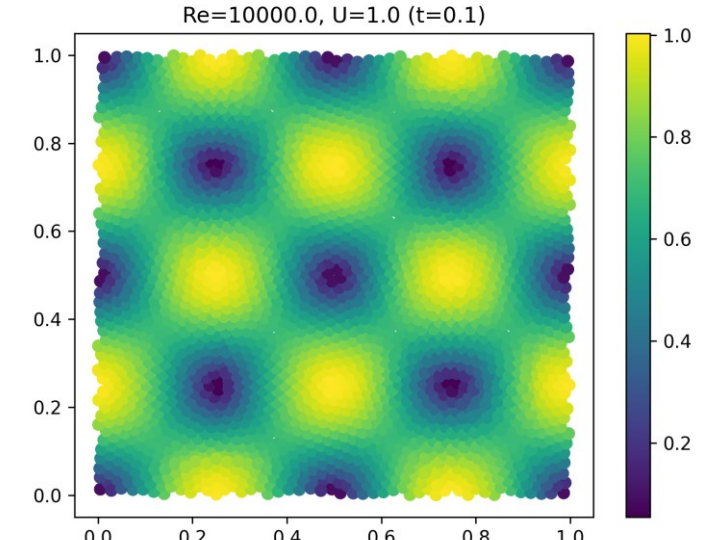


**Fig:** Velocity magnitude field for  $\delta$ -LES-SPH ( $\rho_c$ ) scheme ( $f_{pst} = 10$ ) ( $Re = 10^4, N = 50^2$ )

## Observations

- $\delta$ -LES-SPH ( $\rho_c$ ): Offers better OOC when used with TaitEOS than the other combinations
- $f_{pst}$ : Magnitude of error is least when PST is disabled; but OOC improves with PST

[Go back](#)

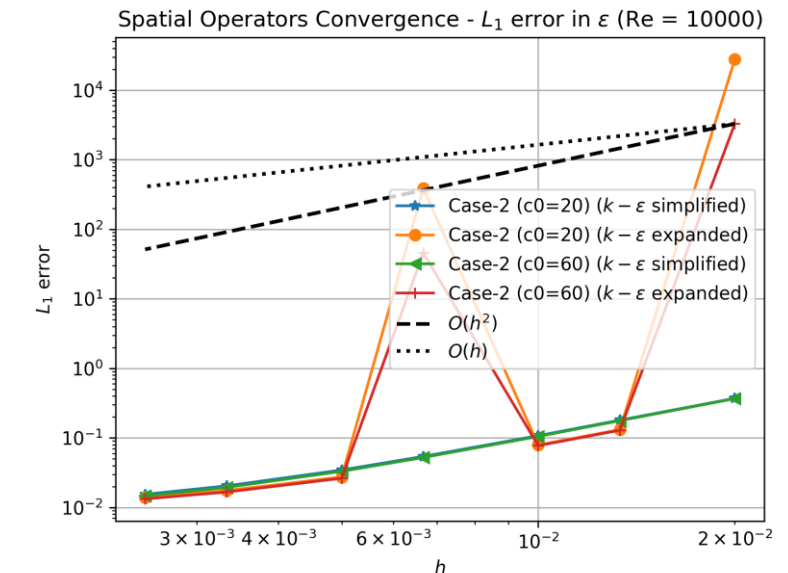
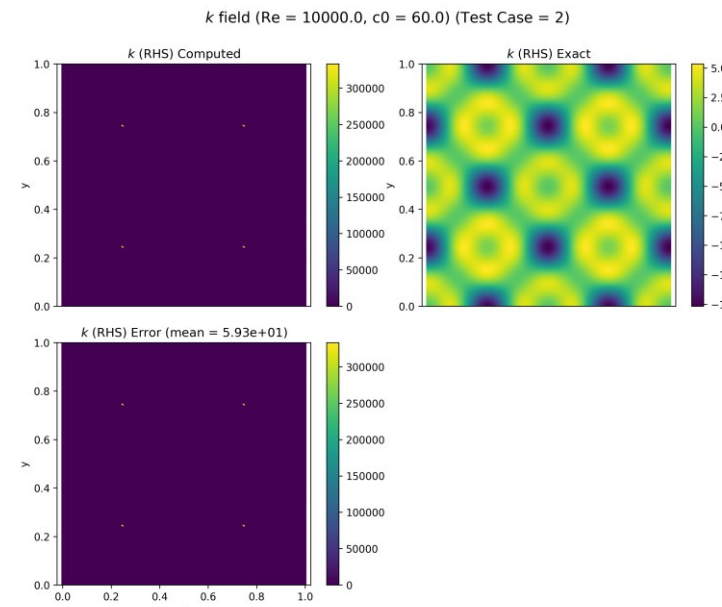
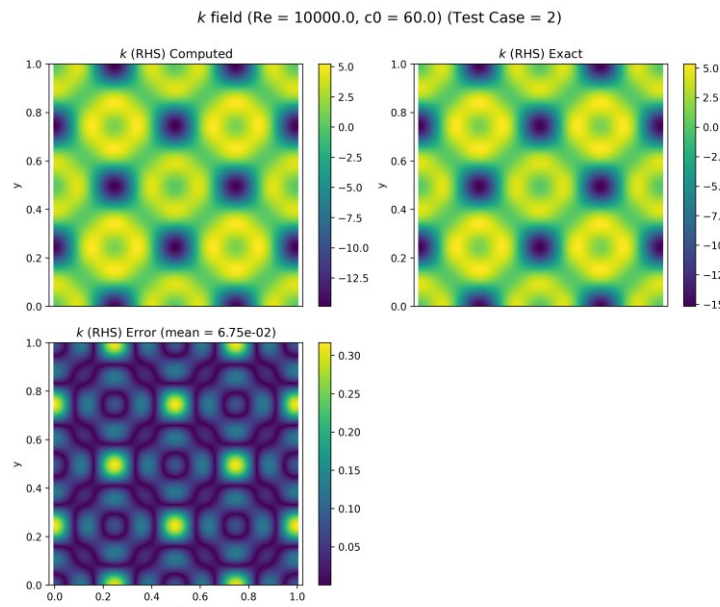
## TaitEOS

$$P_i = P_0 + \frac{\rho_0 c_0^2}{\gamma} \left( \left( \frac{\rho_i}{\rho_0} \right)^\gamma - 1 \right)$$

## LinearEOS

$$P_i = c_0^2 (\rho_i - \rho_0)$$

# RANS-based Model ( $k - \epsilon$ SPH) Analysis



- Simplified eqns.

$$\frac{Dk}{Dt} = \nabla \cdot \left( \frac{\nu_t}{\sigma_k} \nabla k \right) + P_k - \epsilon$$

$$\frac{D\epsilon}{Dt} = \nabla \cdot \left( \frac{\nu_t}{\sigma_\epsilon} \nabla \epsilon \right) + c_{1\epsilon} \frac{\epsilon}{k} P_k - c_{2\epsilon} \frac{\epsilon^2}{k}$$

- Expanded eqns.

$$\frac{Dk}{Dt} = \frac{c_d}{\sigma_k} \left( \frac{k^2}{\epsilon} \nabla^2 k + \frac{2k}{\epsilon} (\nabla k)^2 - \frac{k^2}{\epsilon^2} \nabla k \cdot \nabla \epsilon \right) + P_k - \epsilon$$

$$\frac{D\epsilon}{Dt} = \frac{c_d}{\sigma_\epsilon} \left( \frac{k^2}{\epsilon} \nabla^2 \epsilon + \frac{2k}{\epsilon} \nabla k \cdot \nabla \epsilon - \frac{k^2}{\epsilon^2} (\nabla \epsilon)^2 \right) + c_{1\epsilon} \frac{\epsilon}{k} P_k - c_{2\epsilon} \frac{\epsilon^2}{k}$$

- Test-case 1:  
 $k_0 = 1.5U^2, \quad \epsilon_0 = 0.09^{0.75} \frac{k_0^{1.5}}{L}$
- Test-case 2:  
 $k_0 = |\mathbf{v}_0|^2, \quad \epsilon_0 = k_0$
- Test-case 3:  
 $k_0 = \frac{1}{2} |\mathbf{v}_0|^2, \quad \epsilon_0 = 0.09 \frac{k_0^{3/2}}{L}$

# RANS-based Model ( $k - \epsilon$ SPH) Analysis

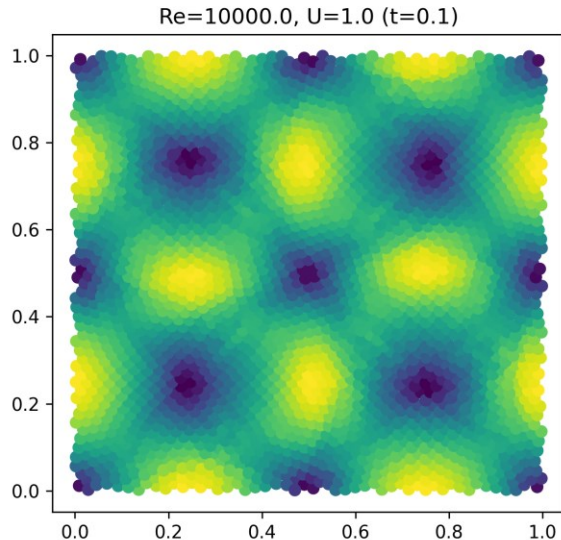


**Fig:** Velocity magnitude field for  $k - \epsilon$  SPH scheme (LinearEOS) ( $Re = 10^4, N = 50^2$ )

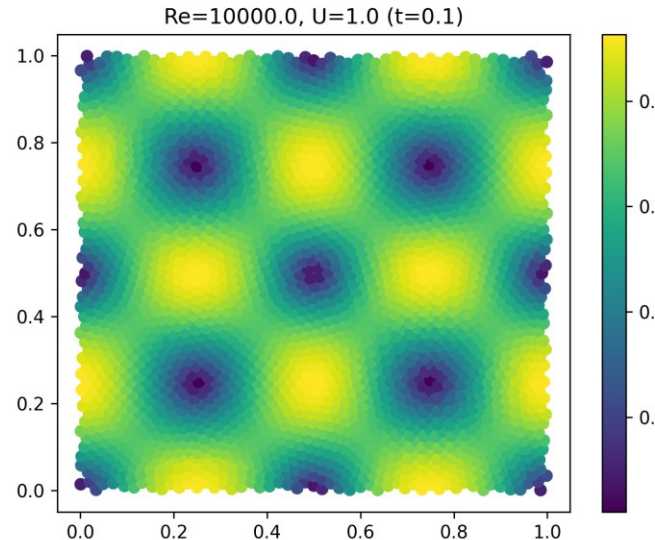


**Fig:** Velocity magnitude field for  $k - \epsilon$  SPH scheme (TaitEOS) ( $Re = 10^4, N = 50^2$ )

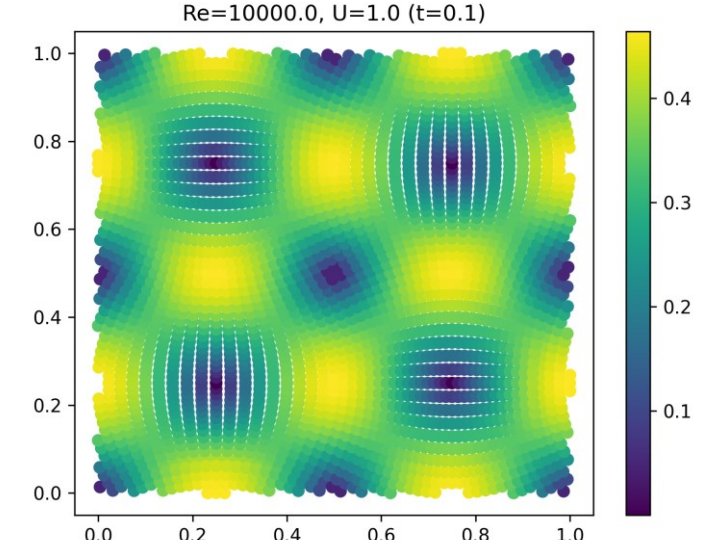


**Fig:** Velocity magnitude field for  $k - \epsilon$  SPH scheme ( $f_{pst} = \text{None}$ ) ( $Re = 10^4, N = 50^2$ )

## Observations

- $k - \epsilon$  SPH discretisation:
  - Variant with simplified transport equations is SOC
  - Increased speed of sound → Improved accuracy
- EOS:
  - Negligible effect on SOC & accuracy
  - TaitEOS better captures the velocity field
- $f_{pst}$ :
  - No effect on the SOC or accuracy of the scheme
  - No PST → Clustering of particles; Domain is no longer uniform

[Go back](#)

# LANS-based Model (SPH- $\epsilon$ ) Analysis

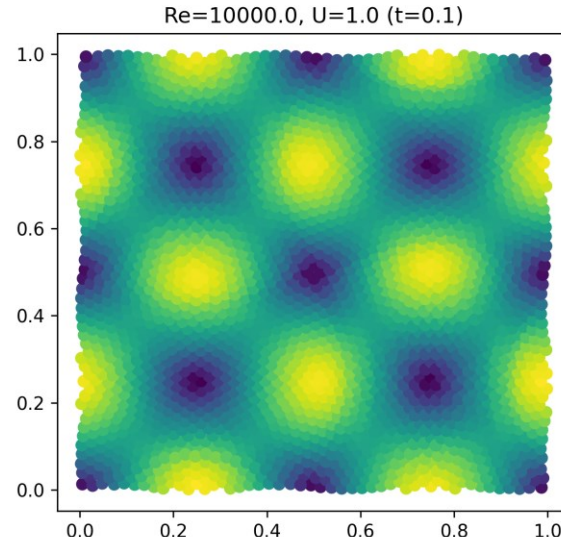


**Fig:** Velocity magnitude field for SPH- $\epsilon$  scheme  
( $\epsilon = 0.5$ ) ( $Re = 10^4, N = 50^2$ )

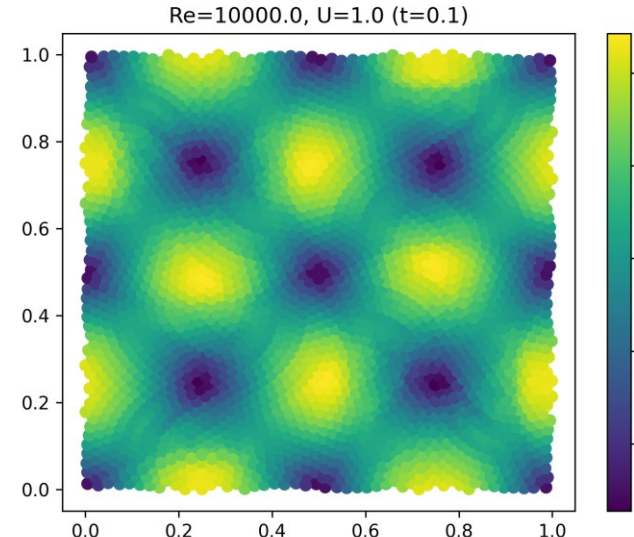


**Fig:** Velocity magnitude field for SPH- $\epsilon$  scheme  
( $\epsilon = 1$ ) ( $Re = 10^4, N = 50^2$ )

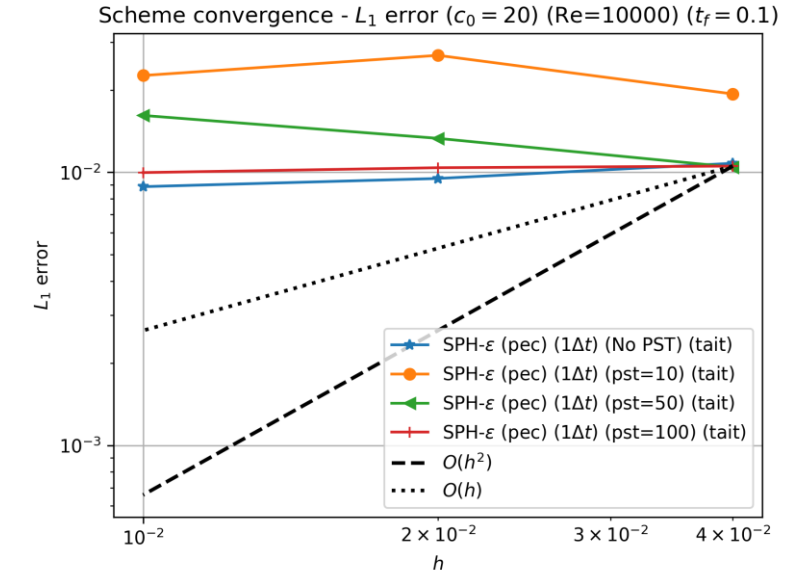


**Fig:** Convergence of the SPH- $\epsilon$  scheme for various  $f_{pst}$  values ( $Re = 10^4$ )

## Observations

- Gradient correction: No effect on the SOC, accuracy, velocity field or energy spectrum of the scheme
- $\epsilon$  : No effect on the SOC or accuracy of the scheme; Increased  $\epsilon \rightarrow$  More diffused velocity field
- EOS: No effect on the SOC, accuracy, velocity field or energy spectrum of the scheme
- $f_{pst}$  :
  - Larger values  $\rightarrow$  Reduced magnitude of  $L_1$  error but no apparent effect on SOC
  - Larger values/No PST  $\rightarrow$  Clustering of particles; Domain is no longer uniform

[Go back](#)

# Appendix B

-- *Additional Turbulence SPH Models* --

# Viscosity-based Models

- Eddy Viscosity Model<sup>[1]</sup>
  - One of the first classes of SPH turbulence models
  - Velocities are Reynolds-averaged
  - First-order closure model:
    - Reynolds stress tensor & mean velocity gradients
  - Turbulent eddy viscosity considered
  - Simulated Poiseuille flow ( $Re = 6.4 \times 10^4$ )

- **Comments**
  - Reproduced log-law profile near walls
  - Appropriate for shear flows

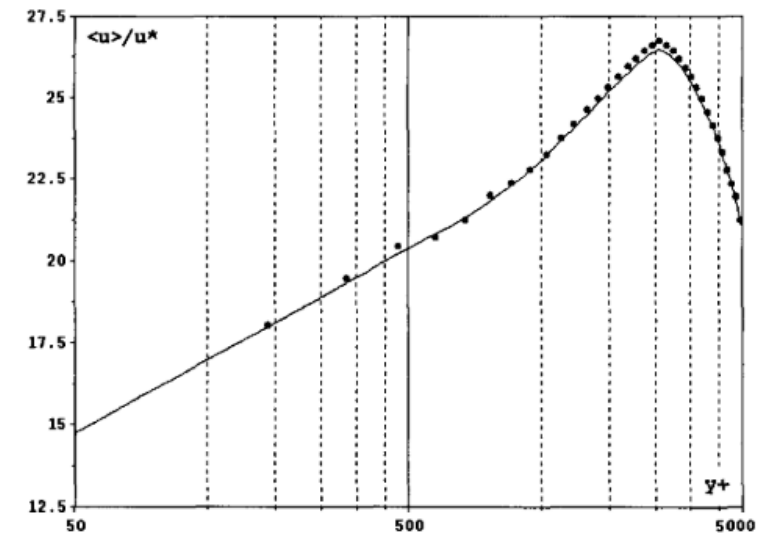


**Fig:** Computed mean velocity profile of turbulent Poiseuille flow in a pipe  
(Rep: Violeau et al)

$$\frac{D \mathbf{v}_i}{D t} = - \sum_j m_j \left( \frac{P_i}{\rho_i^2} + \frac{P_j}{\rho_j^2} + \tilde{\Pi}_{ij} \right) \nabla_i W_{h,ij} + \mathbf{F}_i$$

$$\tilde{\Pi}_{ij} = -8 \frac{\nu_{t,i} + \nu_{t,j}}{\rho_i + \rho_j} \frac{\langle \mathbf{v} \rangle_{ij} \cdot \mathbf{r}_{ij}}{|\mathbf{r}_{ij}|^2 + \xi^2}$$

$$\nu_t = L_m^2 \|\underline{\mathcal{S}}\|_F = L_m^2 \sqrt{\langle \underline{\mathcal{S}}, \underline{\mathcal{S}} \rangle}$$

$$\nabla \langle \mathbf{v} \rangle_i = - \frac{1}{\rho_i} \sum_j m_j \langle \mathbf{v} \rangle_{ij} \otimes \nabla_i W_{h,ij}$$

[1] D. VIOLEAU, S. PICCON, and J.-P. CHABARD, "TWO ATTEMPTS OF TURBULENCE MODELLING IN SMOOTHED PARTICLE HYDRODYNAMICS," in Advances in Fluid Modeling and Turbulence Measurements, Jul. 2002, vol. 1, no. 5, pp. 339–346, doi: 10.1142/9789812777591\_0041.

# Viscosity-based Models

- Generalized Langevin Model<sup>[1]</sup>
  - Prescribed the particle velocity as a random process
  - Acceleration → Function of a random vector (*non-correlated with velocity*)
  - Simulated Poiseuille flow ( $Re = 6.4 \times 10^4$ )

- **Comments**
  - Mean operator appeared to behave like a LES filter
  - Large deviations observed in mean velocity profile ( $\propto k^{0.5}$ )
  - Can be generalized to various types of turbulent flows, & not only shear flows

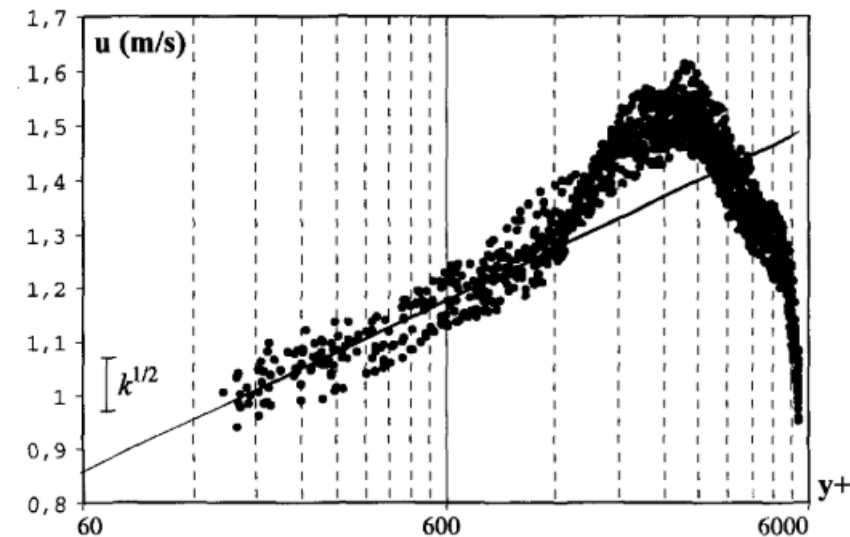


**Fig:** Computed mean velocity profile of turbulent Poiseuille flow in a pipe  
(Rep: Violeau et al)

$$\frac{D \mathbf{v}_i}{D t} = - \sum_j m_j \left( \frac{\langle P \rangle_i}{\rho_i^2} + \frac{\langle P \rangle_j}{\rho_j^2} \right) \nabla_i W_{h,ij} - \frac{1}{2} C_1 \frac{\epsilon_i}{k_i} \mathbf{v}'_i + C_2 \nabla \langle \mathbf{v} \rangle_i \cdot \mathbf{v}'_i + \sqrt{\frac{C_0 \epsilon_i}{\Delta t}} \vec{\xi}_i$$

$$\epsilon_i = 2\nu_{t,i} + \|\underline{S}_i\|_F^2$$

$$k_i = \frac{\epsilon_i \nu_{t,i}}{C_\mu} \quad , \quad C_\mu = 0.009$$

[1] D. VIOLEAU, S. PICCON, and J.-P. CHABARD, "TWO ATTEMPTS OF TURBULENCE MODELLING IN SMOOTHED PARTICLE HYDRODYNAMICS," in Advances in Fluid Modeling and Turbulence Measurements, Jul. 2002, vol. 1, no. 5, pp. 339–346, doi: 10.1142/9789812777591\_0041.

# Viscosity-based Models

- Modified-SPH (mSPH)<sup>[1]</sup>
  - Observation: Absence of viscosity → Noisy particle motion
  - Finite viscosity → Over-prediction of dissipation
  - Modified EOS & MOM eqs. → Particle distribution homogenised
  - Simulated:
    - 2D Taylor-Green Vortex (TGV) ( $Re = \infty$ ,  $N_i = 64^2$ )
    - 3D Taylor-Green Vortex (TGV) ( $Re = 400$ ,  $N_i = 64^3$ )

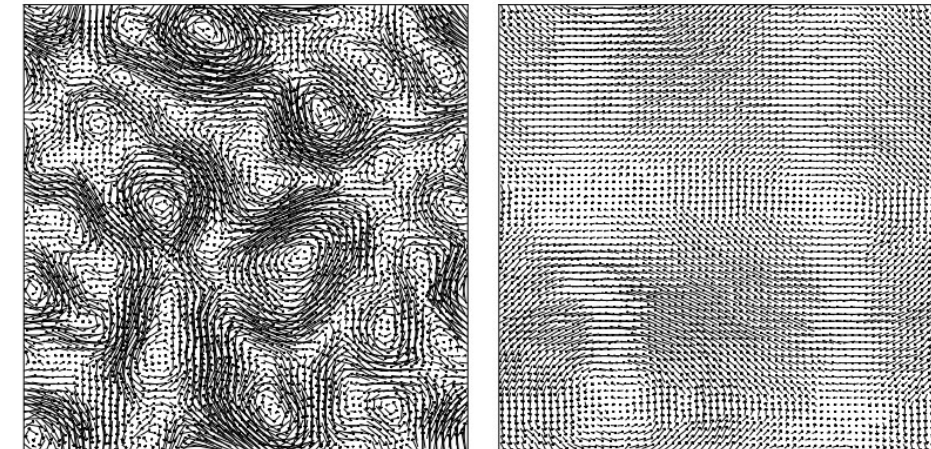


**Fig:** Velocity vector plot at  $t=2$  (left) and  $t=30$  (right). (Rep: Adami et al)

- **Comments**
    - Merging of vortices observed
    - Energy cascade (Kolmogorov scale) slopes reproduced
      - mSPH (-3); standard SPH (1)
    - Transitional flow simulated with reasonable dissipation rate
    - mSPH  $\sim$  Eddy viscosity model below numerical resolution

# Large-Eddy Simulation-based Models

- Implicit Pressure Poisson-based Models<sup>[1,2]</sup>
  - Assumption: Incompressible flow
  - Navier-Stokes (NS) eqs. → Spatially filtered
  - Stress tensor → Closed using Boussinesq's hypothesis
  - Eddy viscosity → Estimated using modified Smagorinsky model
    - Model modified to include wall effects
  - Predictive-corrective time integrator
    - Requires implicit solution of pressure poisson eq
  - Simulated: ( $Re \approx 10^6$ ,  $N_i \approx 10^4$ )
    - 2D wave interaction with partially immersed breakwater<sup>[1]</sup>
    - 2D wave breaking on a beach<sup>[2]</sup>

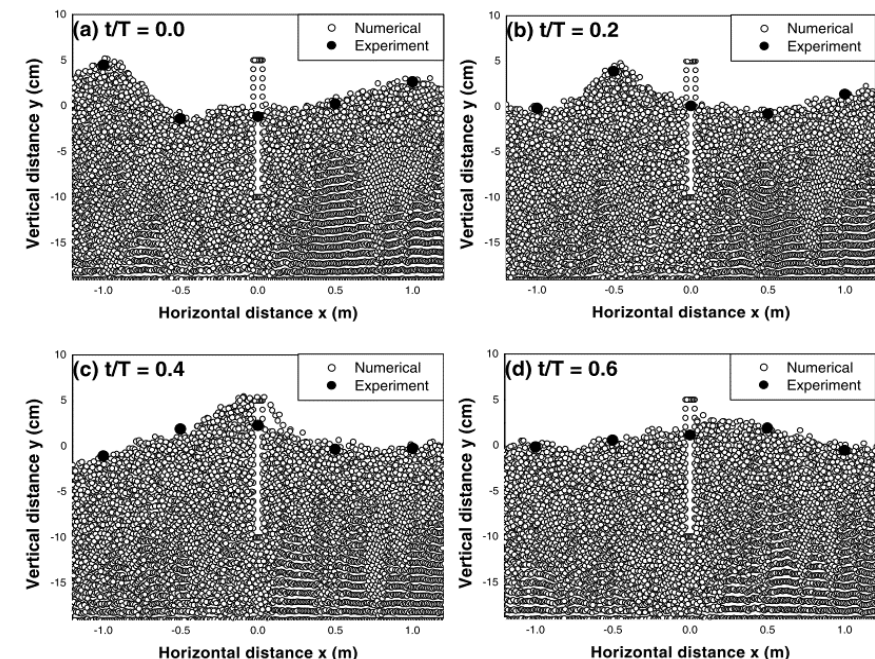


**Fig:** Time sequences of wave profile.  
(Rep: Gotoh et al)

$$\frac{D\bar{\mathbf{v}}}{Dt} = -\frac{1}{\rho}\nabla\bar{P} + \nu\Delta(\bar{\mathbf{v}}) + \frac{1}{\rho}\nabla\cdot\underline{\tau} + \mathbf{F}$$

$$\frac{1}{\rho}\underline{\tau} = 2\nu_t\underline{\mathbf{S}} - \frac{2}{3}k\underline{\mathbf{I}}$$

$$\nu_t = \min(C_s\Delta x, \kappa d_{wall})^2 \sqrt{2\langle \underline{\mathbf{S}}, \underline{\mathbf{S}} \rangle}$$

[1] H. Gotoh, S. Shao, and T. Memita, "SPH-LES model for numerical investigation of wave interaction with partially immersed breakwater," *Coast. Eng. J.*, vol. 46, no. 1, pp. 39–63, 2004, doi: 10.1142/S0578563404000872.

[2] S. Shao and H. Gotoh, "Turbulence particle models for tracking free surfaces," *J. Hydraul. Res.*, vol. 43, no. 3, pp. 276–289, May 2005, doi: 10.1080/00221680509500122.

$$\nabla\cdot\left(\frac{1}{\rho_*}\nabla\bar{P}_{t+1}\right) = \frac{\rho_o - \rho_*}{\rho_o\Delta t^2}$$

# Large-Eddy Simulation-based Models

- Explicit Pressure EOS-based Models<sup>[1,2]</sup>
  - Assumption: Compressible flow
  - NS eqs → Favre averaged
  - Observation: Density variations → Unphysical behaviour on free surfaces
    - Shepard filtering of density performed periodically
  - Simulated: ( $Re \approx 10^6$ ,  $N_i \approx 10^4$ )
    - Weakly plunging breaker in 2D & 3D<sup>[1]</sup>
    - 2D green-water overtopping, 2D & 3D wave breaking, 3D dam break<sup>[2]</sup>

- **Comments**
  - Model predicted regions of high vorticity in 2D
  - Model captured vertically oriented eddies in 3D
  - Accurate for flow separation or splash-based problems
  - Requires large  $N_i$  & very small  $\Delta t$
  - Uncertain regarding scalability to large-scale problems

$$\frac{D\bar{\rho}}{Dt} = -\bar{\rho}\nabla \cdot \tilde{\mathbf{v}}$$

$$\frac{D\tilde{\mathbf{v}}}{Dt} = -\frac{1}{\bar{\rho}}\nabla\bar{P} + \frac{1}{\bar{\rho}}(\nabla \cdot \bar{\rho}\nu\nabla)\tilde{\mathbf{v}} + \frac{1}{\bar{\rho}}\nabla \cdot \underline{\tau} + \mathbf{F}$$

$$\underline{\tau} = \bar{\rho}\left(2\nu_t\underline{\mathbf{S}} - \frac{2}{3}\text{tr}[\underline{\mathbf{S}}]\underline{\mathbf{I}}\right) - \frac{2}{3}\bar{\rho}C_I\bar{\Delta}^2\underline{\mathbf{I}}$$

$$\rho_i = \frac{\sum_j \rho_j W_{h,ij} \mathcal{V}_j}{\sum_j W_{h,ij} \mathcal{V}_j}$$

[1] B. D. ROGERS and R. A. DALRYMPLE, "SPH MODELING OF BREAKING WAVES," in Coastal Engineering 2004, Apr. 2005, pp. 415–427, doi: 10.1142/9789812701916\_0032.

[2] R. A. Dalrymple and B. D. Rogers, "Numerical modeling of water waves with the SPH method," vol. 53, pp. 141–147, 2006, doi: 10.1016/j.coastaleng.2005.10.004.

# Large-Eddy Simulation-based Models

- Explicit Pressure EOS-based Models<sup>[1]</sup>
  - Observation: Standard Smagorinsky model cannot enforce
    - Wall conditions
    - Non-vanishing stresses with laminar flows
  - Devised Wall-adapting local eddy viscosity model (WALE)
  - Simulated an array of cylinders in 2D flow ( $Re \approx 10^2$ ,  $N_i \approx 10^4$ )
- **Comments**
  - LCS captured reasonably well
  - Observed merging of vortices to larger structures
  - Interactions of vortices with opposing strengths → Vorticity cancellation
  - Claim: Complex vortex interactions → Possible difficulty in interpreting the energy spectrum

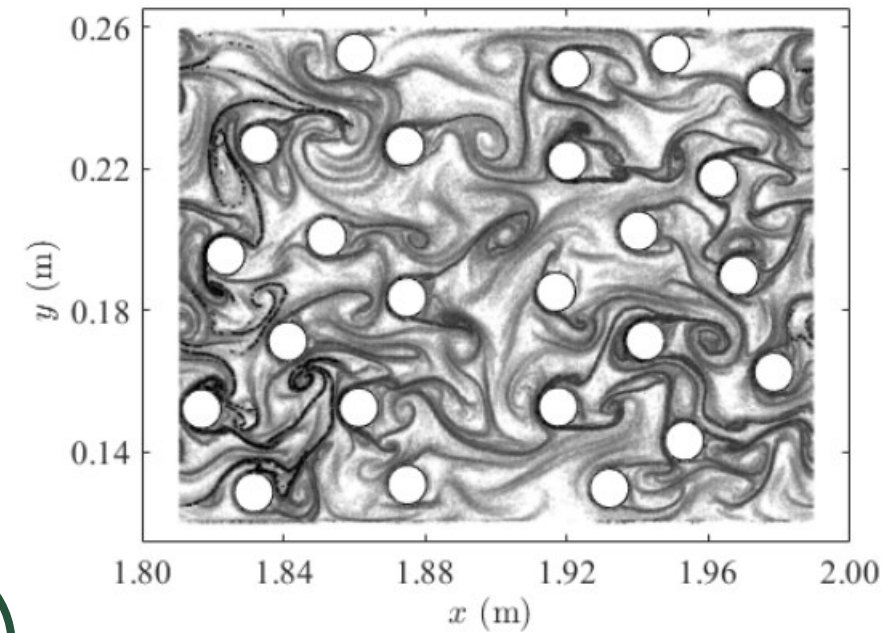


**Fig:** Backward-in-time FTLE field. (Rep: Canelas et al)

$$\nu_t = \rho(C_w \Delta x)^2 \frac{\langle \underline{S}^d, \underline{S}^d \rangle^{3/2}}{\langle \underline{S}, \underline{S} \rangle^{5/2} + \langle \underline{S}^d, \underline{S}^d \rangle^{5/4}}$$

$$\underline{S}^d = \frac{1}{2} \left( (\nabla \mathbf{v})^2 + ((\nabla \mathbf{v})^T)^2 \right) - \frac{1}{3} \text{tr}[(\nabla \mathbf{v})^2] \underline{\mathbf{I}}$$

[1] R. B. Canelas, A. M. Ricardo, R. M. L. Ferreira, J. M. Domínguez, and A. J. C. Crespo, "Hunting for Lagrangian Coherent Structures : SPH-LES turbulence simulations with Wall-adapting Local Eddy Viscosity ( WALE ) model," 11th SPHERIC, no. March 2017, 2016, [Online].

# Miscellaneous Models

- Viscosity-based vorticity correction model<sup>[1]</sup>
  - Aimed primarily towards benefiting the CGI community
    - Faster computational time & simplified system of equations
  - Research focuses more on visual artifacts of the flow, not quantified metrics
  - Builds on the fact that rotational kinetic energy  $\leq$  translational kinetic energy
- Hybrid-SPH (hrSPH)<sup>[2]</sup>
  - Particle data interpolated onto Eulerian mesh grids
  - Rate of change of flow properties computed on mesh grid
  - Updated mesh values interpolated onto particles
  - Advection of particles using the updated properties
  - Remeshing is performed when particles cluster to ensure uniform particle distribution
  - Information from the model cannot help improve traditional SPH schemes

[1] S. Liu, X. Wang, X. Ban, Y. Xu, J. Zhou, and Y. Zhang, "Viscosity-based Vorticity Correction for Turbulent SPH Fluids," in 2019 IEEE Conference on Virtual Reality and 3D User Interfaces (VR), Mar. 2019, pp. 1048–1049, doi: 10.1109/VR.2019.8798224.

[2] A. Obeidat and S. P. A. Bordas, "Three-dimensional remeshed smoothed particle hydrodynamics for the simulation of isotropic turbulence," Int. J. Numer. Methods Fluids, vol. 86, no. 1, pp. 1–19, 2018, doi: 10.1002/fld.4405.

# Benchmark Problems

- Taylor-Green Vortex Problem → Periodic, incompressible flow
  - 2D Case: Analytical solutions known
  - 3D Case: Initial flow conditions can be specified
- Thin Double-Shear Layer
  - Flow under-resolved → Spurious structures are produced
  - Generation of the spurious structure depends on the scheme
- 3D Isotropic Turbulence<sup>[1]</sup>
  - DNS dataset from the JHU Turbulence database Cluster
  - Dataset: Incompressible flow with isotropic and forced turbulence.
  - $1024^3$  spatial points & 1024 time samples spanning one large-scale turnover time
- 2D Confined & Driven Turbulence<sup>[2]</sup>
  - 2D fluid confined to a square box enclosing a cylinder
  - Cylinder moves in a predetermined trajectory

[1] Y. Li et al., "A public turbulence database cluster and applications to study Lagrangian evolution of velocity increments in turbulence," *J. turbul.*, vol. 9, p. N31, 2008.

[2] J. J. Monaghan, "SPH- $\epsilon$  simulation of 2D turbulence driven by a moving cylinder," *Eur. J. Mech. B/Fluids*, vol. 65, pp. 486–493, 2017, doi: 10.1016/j.euromechflu.2017.03.011.